Spring 2011

Shaker table vibration testing of a microsatellite

Tonya Michelle Sanders

Department:

SHAKER TABLE VIBRATION TESTING OF A MICROSATELLITE

by

TONYA MICHELLE SANDERS

A THESIS

Presented to the Faculty of the Graduate School of the

MISSOURI UNIVERSITY OF SCIENCE AND TECHNOLOGY

In Partial Fulfillment of the Requirements for the Degree

MASTER OF SCIENCE IN AEROSPACE ENGINEERING

2011

Approved by

Dr. Henry J. Pernicka, Advisor
Dr. Joshua L. Rovey
Dr. L. R. Dharani

ABSTRACT

In the satellite development process, structural testing is a means to gain confidence in analytical models and ultimately support qualification of the spacecraft for flight. Vibration testing, in particular, is motivated by the safety considerations of crew or launch personnel, the survivability of delicate hardware and electronics, and the avoidance of large stresses that cause structural fatigue or failure. The subject of this thesis is concerned with the shaker table vibration testing of a microsatellite pair designed and built by students at the Missouri University of Science and Technology in Rolla, Missouri. A finite element model (FEM) used in structural response predictions has been formulated for the satellite, and it is the goal of these tests to verify the accuracy of the model and identify any design issues that might result in mechanical or structural damage to the spacecraft or space vehicle during flight. An introduction to environmental vibration research in the space industry is presented, including a discussion of common shaker table tests and equipment, followed by an overview of the satellite test structure. The test philosophy and implementation are introduced, and the results are presented and discussed. To offer insight for future shaker table tests, this thesis concludes with a discussion of the lessons learned.

Results show that the individual microsatellites withstood the shaker excitation input, and can survive the vibration environment during flight. However, significant rattling in the cup / cone interface between the two structures necessitated a redesign of the interface. Potential solutions to this failure mode are discussed.

ACKNOWLEDGMENTS

I would like to thank my advisor, Dr. Henry Pernicka, for his guidance and support during this research and for the exceptional experience of participating in the development of a satellite during college. His instruction provided unique opportunities that helped to make my time at Missouri S&T enjoyable. I would also like to thank my committee members, Dr. Joshua Rovey and Dr. Lokesh Dharani, for the investment of their time, as well as their efforts on behalf of my education.

Financial support, including the graduate teaching program at Missouri S&T, is gratefully acknowledged.

The members, both past and present, of the Missouri S&T Satellite Team deserve much appreciation for their contributions to this program. Thank you to members of the Structures subsystem who were involved in the shaker table tests and to Mr. Brad Fink and Mr. Rick Campen from Caterpillar in Peoria, Illinois, who graciously offered of their time and expertise. The tests would not have been accomplished without their efforts.

I would like to thank my family for their support and guidance throughout the years. I am grateful for all they do to help me accomplish my goals and for their encouragement to overcome any challenges.

Finally, I would like to thank God for providing me with fortitude and perseverance during college and for the blessing of working on exciting research projects, meeting people who challenged me to grow, and graduating with wonderful memories from once-in-a-lifetime experiences.

TABLE OF CONTENTS

Page

ABSTRACT iii

ACKNOWLEDGMENTS iv

LIST OF ILLUSTRATIONS viii

LIST OF TABLES x

SECTION

1. INTRODUCTION 1

1.1. STRUCTURAL VIBRATION IN SPACECRAFT 2

1.2. ENVIRONMENTS CONTRIBUTING TO VIBRATION 3

1.2.1. Random Loads. 5

1.2.2. Acoustic Loads. 5

1.2.3. Sinusoidal Loads. 6

1.2.4. Shock Loads. 6

1.2.5. Transportation Loads. 6

1.3. AEROSPACE VIBRATION TESTING 6

1.4. PURPOSE 13

1.5. THESIS ORGANIZATION 14

2. BACKGROUND 15

2.1. VIBRATION TEST INSTRUMENTATION 15

2.2. VIBRATION TESTS 16

2.2.1. Sine Vibration Tests. 16

2.2.2. Random Vibration Tests. 18

2.2.3. Combined Vibration Tests. 19

2.3. PURPOSE AND COMPARISON OF TESTS 19

2.3.1. Qualification for Flight Environments. 20

2.3.2. Failure Identification. 20

2.3.3. Workmanship Tests. 20

2.3.4. Model Verification. 21

2.3.5. Test Advantages and Disadvantages. 21

2.3.6. Control and Limiting of Vibration Tests. 21
2.4. TEST PLAN DEVELOPMENT AND IMPLEMENTATION 22
2.4.1. Requirements Definition. 22
2.4.2. Pre-Test Analysis. 23
2.4.3. Preparation of the Written Test Plan. 24
2.4.4. Hardware Definition. 24
2.4.5. Facilities and Personnel. 24
2.4.6. Fixtures. 25
2.4.7. Instrumentation. 25
2.4.8. Test Options and Test Sequence. 25
2.4.9. Equipment Operation and Control. 26
2.5. RESULTS INTERPRETATION 26
2.5.1. Structural Integrity. 27
2.5.2. Post-Test Analysis. 27
2.5.3. Design Iterations and Retests. 28
2.5.4. Verification and Validation. 28
3. TEST STRUCTURE OVERVIEW 29
3.1. M-SAT MISSION SUMMARY 29
3.2. STRUCTURAL DESIGN CONSTRAINTS 30
3.3. M-SAT TEST STRUCTURE 31
3.3.1. Primary Structure. 31
3.3.2. Spacecraft Components. 34
3.4. TEST SPACECRAFT CONFIGURATION 36
3.4.1. Dimensions. 36
3.4.2. Mass Properties. 38
3.4.3. Satellite Interfaces. 40
3.4.4. Satellite Configurations. 41
4. TEST PLAN AND IMPLEMENTATION 44
4.1. TEST SPECIFICATIONS 44
4.1.1. Sine Sweep. 44
4.1.2. Sine Burst. 44

4.1.3. Random Vibration. 44
4.2. TEST SEQUENCE 45
4.3. EQUIPMENT AND HARDWARE 47
4.4. DATA ACQUISITION 52
4.5. TEST PROCEDURES 56
5. RESULTS 58
5.1. MR SAT 58
5.1.1. Z-Axis Swept Sine. 58
5.1.2. Z-Axis Sine Burst. 59
5.1.3. Z-Axis Random Vibration. 60
5.1.4. X-Axis Swept Sine. 61
5.1.5. X-Axis Sine Burst. 61
5.1.6. X-Axis Random Vibration. 62
5.2. MRS SAT 62
5.2.1. Z-Axis Swept Sine. 62
5.2.2. Z-Axis Sine Burst. 62
5.3. MR AND MRS SAT DOCKED 63
5.4. FINITE ELEMENT ANALYSIS COMPARISON 63
6. CONCLUSION 65
6.1. LESSONS LEARNED 65
6.1.1. Fixture Design. 65
6.1.2. Equipment Operation. 66
6.1.3. Design Iterations. 66
6.2. CONTINUING WORK 67
6.3. CLOSING REMARKS 68
APPENDIX 69
BIBLIOGRAPHY 76
VITA 78

LIST OF ILLUSTRATIONS

Figure Page

1.1. First Rocket Test Stand Used in Vibration Testing 8
1.2. Test Facility Block House 8
1.3. Propulsion System Firing of the Saturn 1C 9
1.4. Space Shuttle Enterprise in the Dynamic Test Stand..... 10
2.1. Typical Shaker Table Set-Up 15
3.1. MR SAT and MRS SAT In-Flight Formation 29
3.2. MR SAT Structure.....32
3.3. MRS SAT Structure 32
3.4. MR SAT Isogrid Panel 33
3.5. MR SAT Isogrid Panel 33
3.6. MR SAT Brackets..... 34
3.7. MR SAT Overall Dimensions 37
3.8. MRS SAT Overall Dimensions 37
3.9. Docked Configuration Overall Dimensions 38
3.10. Spacecraft Reference Frame 39
3.11. MR and MRS SAT Mechanical Interface 40
3.12. MR SAT Configuration 41
3.13. MR SAT Flowered View 42
3.14. MRS SAT Configuration 42
3.15. MRS SAT Flowered View 43
4.1. Nanosat Random Vibration Test Levels 45
4.2. AFRL Environmental Test Flow 46
4.3. MR SAT (Left) and MRS SAT Shown Mounted to the Shaker Table 47
4.4. Rotating the Shaker Table for X- and Y-Axis Tests 48
4.5. Commercial Electrodynamic Shaker 49
4.6. Isometric View of MR SAT Shaker Mounting Fixture 50
4.7. Isometric View of MRS SAT Shaker Mounting Fixture 50
4.8. MR SAT Mounting Locations 51

4.9. MRS SAT Mounting Locations 52
4.10. Accelerometer Mounted to the Battery Box on MR SAT Panel 2 54
4.11. Accelerometer Mounted to the Propulsion Tank Mass Simulator on MR SAT 54
4.12. Accelerometer Mounted to the QwkNut 3K Mass Simulator on MR SAT..... 55
4.13. Accelerometer Mounted to the Battery Box Mass Simulator on MRS SAT 55

LIST OF TABLES

Table Page

1.1. Sources of Vibration in Vehicle Operational Phases 4

2.1. Sample Random Vibration Test Environment 18

3.1. M-SAT Mission Constraints 30

3.2. M-SAT Component List by Subsystem 35

3.3. MR SAT Mass Properties 38

3.4. MRS SAT Mass Properties 39

3.5. Docked Configuration Mass Properties 39

4.1. Nanosat-6 Random Vibration Spectrum Test Levels 45

1. INTRODUCTION

The life of a space vehicle is characterized by complex and physically stressful environments. During lift-off and ascent into orbit, when conditions are most extreme, the system of launch vehicle and payload operate under intense acoustic noise, broad temperature gradients, aerodynamic buffeting, shock loads, and vibration. Despite the wealth of historical spaceflight data available, the unique nature of launch conditions presents a challenge in mission planning. Every new component, new process, or new technology introduces uncertainty in the prediction of and structural response to dynamic loading environments.

In the satellite development process, structural testing is a means to gain confidence in analytical models and ultimately support qualification of the spacecraft for flight. A typical structural test plan might incorporate [1]:

- A static test to qualify the strength adequacy of the primary structure and its critical interface points;
- A modal survey or sine vibration test to determine natural frequencies of the structure (at which it will exhibit a large amplitude of motion for a small input force), its mode shapes, and damping characteristics;
- A shock test to simulate launch vehicle staging;
- An acoustic test or random vibration test to support verification of the spacecraft against the intense acoustic pressure loads during launch and ascent;
- And sine vibration tests to qualify the adequacy of the structure when exposed to excitation from the launch vehicle.

This thesis study centers on the vibration problem in spacecraft structures as it relates to the design process and standard practices for structural qualification and acceptance testing.

1.1. STRUCTURAL VIBRATION IN SPACECRAFT

Concern for vibration and vibroacoustic phenomena in spacecraft and their launch systems has several motivations: safety considerations for crew or launch personnel, the survivability of delicate hardware and electronics, structural fatigue prevention, and the avoidance of large stresses that cause structural deformation. Acoustic pressure loads, particularly those resulting from the operation of space vehicle propulsion systems, are a major component of the structural vibration problem. In the 1981 maiden flight of NASA's Space Shuttle, the primary mission goals were to accomplish a safe ascent into orbit, check out the systems onboard, and return safely to Earth. All major objectives were met successfully, and the worthiness of the Shuttle as a space vehicle was verified. A post flight inspection, however, revealed that an overpressure wave had occurred when the solid rocket boosters ignited. The intense acoustical energy reflected by the launch structure exerted significant force on the wing and control surfaces of the Orbiter, resulting in the loss of 16 heat shield tiles and damage to 148 others [2].

In the history of space vehicle design, vibration loads have caused concern or failure in the following additional circumstances [3]:

- The effects of torsion vibration during staging of a major launch vehicle required careful consideration of payload torsion characteristics to minimize loads and accelerations on the spacecraft structure;

- Control-system coupling with a launch vehicle structure in the launch mode led to engine shutdown to prevent failure from vibration;

- Pogo-type longitudinal vibration, brought on by the unstable coupling of the propulsion system with the longitudinal structural vibration, caused excessive loads, resulting in booster malfunction;

- Inadequate analysis during the design phase has frequently resulted in overstressing and failure during prototype spacecraft testing.

Given the oscillatory nature of these responses, severe structural vibration will likely cause fatigue damage. Thus, it becomes imperative to identify the situations that trigger excessive motions in the spacecraft structure. While not all vibratory loads will result in damage, in the case of manned space vehicles, it might be necessary to address vibratory responses as a source of discomfort or impedance to the crew. For example, while developing the Ares I rocket in 2008, engineers discovered vibrations up to 0.5 g inherent in the solid rocket boosters. For a few critical seconds during launch, the vibrations would have limited the crew members' abilities to function and read instrument data [4].

To consider properly the effects of vibration on a space structure, the external loads, both naturally occurring and induced, must be defined accurately. A projection of these loads is of great importance to the determination of vibration test environments. Then, margins of safety can be incorporated into the structural design, and a model can be generated for use in response predictions.

1.2. ENVIRONMENTS CONTRIBUTING TO VIBRATION

There are three basic types of loading environments present during flight [5]:

- Low-frequency sinusoidal vibration, typically from 5 Hertz (Hz) to 100 Hz, resulting from transient flight events;

- High-frequency random vibration, which typically has significant energy in the frequency range from 20 Hz to 2,000 Hz;

- High-frequency acoustic pressure, typically 20 Hz to 10,000 Hz, inside the payload compartment.

Also, the spacecraft will encounter very short duration transients, known as shock loads, when separating from the launch vehicle, at engine ignition or shutdown, or during vehicle staging. Combinations of these environments occur at different times. Table 1.1 lists the operational phases of a space vehicle and the possible sources of vibration in each phase.

Table 1.1. Sources of Vibration in Vehicle Operational Phases [1],[3]

Operation	Phase	Source	Loading Environment			
			Acoustic	Random Vibration	Sine Vibration	Shock
Launch	Lift-off	Ignition, Engine noise, Tie-down release	x	x		x
	Ascent	Engine roughness, Aerodynamic noise / buffet, Motor burn / Combustion / Pogo, Control-system instability	x	x	x	
	Staging	Separation, Stage ignition				x
Space	On orbit	Extension of folded elements (i.e. solar panels)			x	
	On station	Control-system instability			x	
Atmospheric	Re-entry	Aerodynamic noise / buffet, Aerodynamic instability	x	x		

Not all mechanical loads are equally important; rather, they depend on the type of structure under consideration, such as the primary structure (i.e. support panels) or the secondary structure (i.e. solar panels, antennas, instruments, and electronic boxes.) For example, secondary structures with large surface areas, such as solar panels, are particularly sensitive to random vibration. Furthermore, the loads encountered during flight depend not only on the external environment, but also on the structural properties of the spacecraft. For instance, the magnitude of loads transmitted from the launch vehicle to the payload is a function of both the vehicle design and the launch configuration.

1.2.1. Random Loads. In the payload compartment of the launch vehicle, intense acoustic pressure impedes on the outside panels of spacecraft and is converted into mechanical random vibrations that cause both the panels and the secondary structures mounted on them to vibrate. Instruments and electronics are fairly sensitive to this environment. Random loads are also transmitted from the launch vehicle to the base of the payload spacecraft, brought on by acoustic loads and boundary layer turbulence.

The random vibration frequency domain lies in the range of 20 Hz to 2000 Hz for nearly all launch vehicles. However, if a structural response analysis is carried out over the high-frequency bands of random loads, finite element or boundary element methods prove insufficient. In general, the reliable upper limit of the frequency domain for complex finite element models in 200 Hz to 300 Hz. It thus becomes necessary to rely on a statistical approach when performing the analysis as a complement to the finite element or boundary element methods.

1.2.2. Acoustic Loads. The rocket engines, the separation of airflow along the launch vehicle, and the aerodynamic noise during flight contribute to this loading environment in a broad frequency spectrum from 20 Hz to 10,000 Hz. Acoustic loads peak during liftoff, when noise levels on the launch pad approach 150 decibels. The result induces vibration not only of the space vehicle, but also of the launch tower and surrounding support facility. In the payload compartment, acoustic loads are transmitted by direct impingement on the surfaces of exposed components and by impingement on component mounting structures. Loads on these mounting structures generate random vibrations that are mechanically transmitted to the spacecraft components. The acoustic pressure peaks again during transonic flight and at maximum dynamic pressure, generating similar vibrations in the payload.

As with random loads, there are limitations to analytical predictions for acoustic environments. If the structural response calculations are carried out over the entire frequency domain of acoustic loads (up to 10,000 Hz), the finite element method is insufficient. Statistical methods must again be applied if a reliable prediction is to be achieved.

1.2.3. Sinusoidal Loads. Low-frequency sinusoidal loads result from the interaction between the launch vehicle mode shapes and the loads generated by: 1) liftoff, when the fast build-up of thrust induces a shock load that excites the low-frequency domain; 2) combustion of the engines, which results in sinusoidal vibrations occurring both in, and adjacent to, the launch direction; and 3) pogo-like vibrations, observed just before the burn-up of a stage.

1.2.4. Shock Loads. The separation of stages and the separation of the spacecraft from the launch vehicle induce very short duration loads in the internal structure of the spacecraft, known as shock loads. Their duration is very short with respect to the duration associated with the fundamental natural frequencies of the system. The effects of the shock loads are usually depicted in a shock-response spectrum (SRS). The SRS is essentially a plot that shows the responses of a number of single degree of freedom (SDOF) systems to an excitation. Since an SRS has no time history, it cannot be simulated using a shaker table. There is a method to calculate a time history from a given SRS; but the resulting time history is not unique, and arriving at the correct SRS is a process of trial and error. Determining a time history also depends greatly on the physical limitations of the shaker table.

1.2.5. Transportation Loads. Spacecraft also may be exposed to dynamic loads, such as shocks and random vibration, during their transportation between the design facility and the launch site. Transportation limit load factors are established during the design phase to protect against any damage. These environments are, by design, generally less severe than launch loads, but should be included in the design analysis unless special protection is provided to insure that they contribute negligible damage compared with flight loads [1].

1.3. AEROSPACE VIBRATION TESTING

Vibration testing has existed since the early days of aircraft design and production, but its processes matured significantly with the introduction of jet propulsion. Since the vibration environment of early piston-engined aircraft was primarily tonal, sine testing and swept sine testing could closely simulate actual flight conditions. Jet-powered aircraft, however, fly at higher speeds where aerodynamic forces generate

broadband vibration, so it became necessary for the testing requirements and technologies of the time to evolve dramatically. Consequently, while innovations in several other areas of environmental testing were later necessary to qualify components exposed to the extreme conditions of space, the dynamics test field needed only minor adjustments. By the time Sputnik I launched in 1957, the aeronautics industry had in place advanced methods of vibration, shock, and aerodynamic testing [6].

Following World War II, a team of scientists and engineers working under the U.S. Army's Redstone Arsenal in Huntsville, Alabama, became prominent figures in America's fledgling space program. Between 1950 and 1956, the Development Operations Division of the Army Ballistic Missile Agency designed the first Redstone and Jupiter C rockets, as the Soviet Union was simultaneously developing the R-7, which on October 4, 1957, would launch the first artificial satellite into orbit. With this satellite, Sputnik I, the Soviets ushered in the era of space exploration. Weighing 83.6 kilograms and equipped only to transmit radio signals to Earth, its simple design was selected in favor of more complicated satellites to expedite launch [7]. Shortly thereafter, on January 31, 1958, the U.S. launched its Explorer I satellite using a Jupiter C rocket. The primary science experiment onboard, provided by Dr. James Van Allen of the University of Iowa, was a cosmic ray detector designed to measure the radiation environment in Earth orbit. After its instruments detected a much lower cosmic ray count than expected, Van Allen theorized the existence of radiation belts trapped by Earth's magnetic field, which were later verified and named in his honor [8].

The Jupiter C, retroactively named the Juno I, was a modified Redstone rocket. Since it was designed to propel conventional or atomic warheads, the Redstone was required to be an extremely accurate and reliable missile, and its propulsion and guidance systems underwent an extensive inspection and test program at the Army's Redstone Arsenal. Construction of the first rocket test stand was completed in 1953, and the first test firings of the Redstone were held in April of the same year. The stand, shown in Figure 1.1, measures 75 feet in height and is 33 feet by 22 feet at its concrete base. The block house in Figure 1.2 was used for observations and receiving telemetered data during the tests, and was constructed from three surplus chemical steel tanks, which were covered on the outside by dirt. These humble test grounds stemmed from an inflexible

law stating that no funds for research and development could be spent on facility construction. Rather than waiting for funding, Redstone engineers designed the interim test stand for $25,000, which was the maximum amount allowed without Congressional approval.

Figure 1.1. First Rocket Test Stand Used in Vibration Testing [9]

Figure 1.2. Test Facility Block House [9]

Before each test firing, an instrumentation crew placed transducers at strategic locations within the rocket. Data from the transducers traveled along cables to an instrumentation tank, and provided a record of critical temperatures, pressures, flow-rates, and vibrations during the run. For the first two years, test runs lasted no more than 15 seconds, but after expansion and strengthening of the stand, some runs lasted up to 120 seconds [9].

Similar programs were conducted on the Soviet R-7 rocket. By March 20, 1956, a three-stage development test plan was established, calling for two lots of prototype rockets for stand tests and one lot for flight tests. Necessary changes would be incorporated into a subsequent lot of rockets, and a final lot would be issued that represented the flight tested iterated configuration [10].

In 1957, the Solid Rocket Motor Structural Test Facility was constructed by the U.S. Army at what would later be named the George C. Marshall Space Flight Center. The test stand, shown in Figure 1.3, measures 175 feet in height, and is 20 feet by 30 feet at its base. One side of the two-position stand has been modified to support solid rocket booster static testing. The facility, which has been preserved as a national historic landmark, is still active and capable of providing support for the development and testing of new rocket vehicles [11].

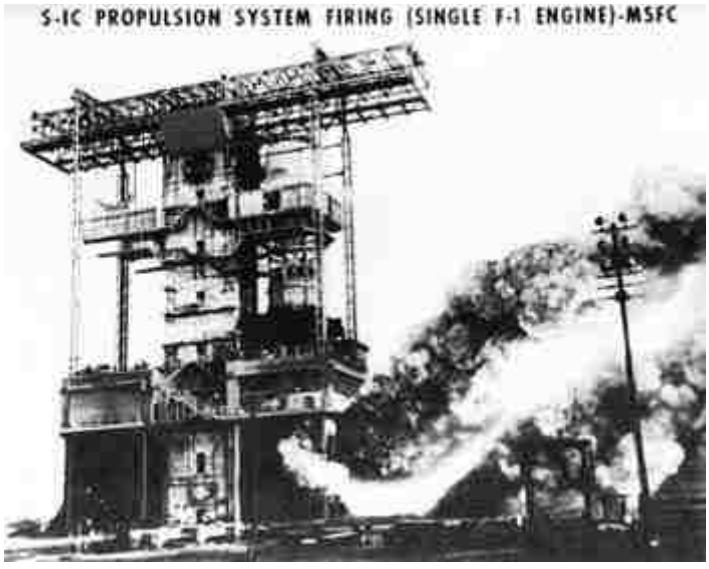

Figure 1.3. Propulsion System Firing of the Saturn 1C [11]

In 1964, a dedicated dynamic test stand was constructed at Marshall Space Flight Center to conduct mechanical and vibration tests on the fully assembled Saturn V rocket. The Saturn V, which was used in the Apollo and Skylab programs, was one of the most reliable launch vehicles ever built. This was due in part to the implementation of stringent reliability and quality assurance programs in its manufacturing processes, as well as an exhaustive ground test program.

The dynamic test stand measures 360 feet in height and 122 feet by 98 feet at its base. During testing, the vehicle rests on hydrodynamic supports that provide a maximum of six degrees of freedom of movement. Vibration loads can be induced in the pitch, yaw, or longitudinal axis to obtain resonant frequencies and bending modes [12].

After completion of the Saturn V program, the stand was modified for use in dynamic tests of the Space Shuttle. Figure 1.4 shows the Orbiter Enterprise being hoisted into the stand in 1978 for the Mated Vertical Ground Vibration Test (MVGVT), marking the first time that the Orbiter, External Tank (ET), and two Solid Rocket Boosters (SRB) were mated together. Most recently, the facility was used in dynamic tests of the Ares I launch vehicle [13].

Figure 1.4. Space Shuttle Enterprise in the Dynamic Test Stand [13]

The vibration testing of payload spacecraft evolved significantly under the Apollo program. In the early years of un-manned flight, high priority went to setting up a program for the one-time qualification of a component or system design and to overseeing manufacturer execution of the program. These qualification tests factored in the expected environments during storage, transportation and handling, ground-test duty cycles, and two-mission duty cycles. After the un-manned flight program began, actual measurements were used in adjusting vibration qualification levels.

Even with this exacting program, however, many experienced engineers believed that every piece of flight hardware should be required to pass some environmental testing before being accepted for installation in the space vehicle. Thus, nearly all functional equipment underwent acceptance testing; however, most of these tests were left to the individual designers and systems engineers. In general, the components and systems were limited to complete functional bench tests at room temperature and pressure and a survival test after a brief exposure to random vibration in the axis suspected of being the most sensitive. Unfortunately, the expected vibration levels were so low in many cases that tests failed to reveal workmanship and manufacturing errors, some of which came to light late in the program, leading to delays.

Following the Apollo 1 fire, which occurred in the command module during a launch pad test in 1967, NASA initiated an extensive review of its acceptance test practices. Subcontractors and vendors representing a cross-section of electrical, electronic, and electromechanical equipment throughout the spacecraft received questions regarding their individual acceptance test plans and objectives. This survey revealed the inadequacy, or in many cases, the non-existence of environmental acceptance tests. A decision was made by NASA to review in earnest all Apollo spacecraft acceptance, checkout, and pre-launch test plans and procedures.

The results showed that, in general, factory checkout and pre-launch test tolerances were adequate. Between installation and launch, the equipment passed the same tests several times. The revised overall test requirements, which came out of the review, resulted in a more efficient test plan from pre-delivery acceptance tests to launch. For the development of the Lunar Module (LM), NASA ruled that a component should withstand vibration levels in each of three mutually perpendicular axes for a minimum of

one minute and a maximum of five minutes. A firm ground rule also required that the minimum qualification vibration level be 1.66 times greater than the acceptance test level at all frequencies; although, the acceptance test levels were still very low. In addition, testers had to monitor all pilot-safety functions and check all electric paths for continuity and short circuits. Originally, there were acceptance test plans for approximately 150 LM items; 80 were altered significantly [14].

For the first 50 years of space travel, conventional methods for vibration testing remained similar. However, they often proved ill-suited for lightweight and sometimes delicate aerospace equipment. In recent years, the increased use of optical components has levied a new set of cleanliness requirements on environmental test laboratories. During the fabrication and test programs for the Hubble Space Telescope, many new innovations were necessary due to the contamination control requirements developed by the project scientists. Even a shaker table located in a class 10,000 clean room is surrounded by enough oil vapors in its vicinity to contaminate sensitive optical equipment. To prevent this occurrence during vibration testing, articles can be wrapped in clean static dissipative material while a purge of high purity nitrogen gas is introduced [6].

In some cases, vibration test levels have been too demanding, and equipment that could have survived spaceflight has failed during ground tests. To address this problem, NASA flew the Shuttle Vibration Forces (SVF) experiment onboard STS-90 in 1998, and again onboard STS-96 in 1999, to measure the dynamic forces between the Shuttle and a standard getaway special (GAS) canister attached to the Orbiter's payload bay wall. SVF was designed to validate, what was at the time, a new vibration test method that involved limiting the force of the shaker table test to the force expected during flight. The procedure of force limiting makes vibration tests more realistic by simulating the impedance characteristics of the mounting structure during shaker table testing, and as a result, would enable NASA to fly more sophisticated equipment on Space Shuttle missions. Commercial tri-axial force transducers were incorporated into four custom brackets, which replaced the brackets ordinarily used to attach a GAS canister to the Orbiter's sidewall, and two accelerometers along with signal processing and recorders were located within the canister. The SVF experiment was a self-supporting payload,

meaning it was battery-powered, and the data was recorded within the payload without the need for crew interface. The SVF payload was activated automatically by Orbiter liftoff vibrations and operated for approximately 240 seconds. Results from the second SVF experiment validated the methods being used by NASA for force limiting [15].

Today, spacecraft assembly, integration, and test are driven more and more by production demands. Especially in the case of distributed space systems, where multiple spacecraft must undergo vibration testing within the same program, the approach in test set-up, procedures, and collection and analysis of results must be redefined to optimize the time and resources available. Streamlining the test flow might involve using more than one shaker table to perform dedicated activities, or combining acoustic and vibration tests to reduce the time and manpower devoted to configuration and handling.

The roles of test and analysis should be viewed as complementary. As testing tends to be expensive and time-consuming, it is important to use analysis in the planning stages to improve efficiency, and afterward, to extend the results to other loading and hardware configurations. An adequate mathematical model is of great importance to the prediction of displacements, loads, and stresses resulting from vibratory inputs to the structure, and also provides test operators with an idea of potential risks. Moreover, analytical models are useful in the initial design stages, as they save time, and pose no risk to equipment or resources.

Given these benefits, in the present culture of "faster, better, cheaper," there is a trend in the aerospace industry to rely more on analysis and less on structural tests. It is anticipated that test results will verify analytical predictions, but often this is not the case. Experience has shown that only a well-balanced test program can instill confidence in delivered hardware.

1.4. PURPOSE

The subject of this thesis is concerned with the shaker table vibration testing of a microsatellite structure designed and built at the Missouri University of Science and Technology (Missouri S&T) in Rolla, Missouri. The satellite placed third out of eleven entries in the 2007 University Nanosat Program (UNP) Nanosat-4 competition, and some of its secondary structure and original components were incorporated into an iterated

design for the 2011 Nanosat-6 campaign. The UNP is a two-year cyclic competition sponsored by the Air Force Research Laboratory (AFRL), Air Force Office of Scientific Research (AFOSR), and the American Institute of Aeronautics and Astronautics (AIAA). The winning spacecraft from the competition is eligible for a launch opportunity with the Department of Defense (DoD) Space Test Program (STP).

A finite element model used in structural response predictions has been formulated for the Nanosat-4 satellite, and it is the goal of these tests to verify the accuracy of the model and identify any design issues that might have led to mechanical or structural damage to the spacecraft or space vehicle during flight. To this end, the following tests were conducted:

- **Sine Sweep** to demonstrate the fixed-base natural frequency of the satellites and to detect structural damage during testing, should any occur;
- **Sine Burst** to induce the quasi-static qualification loads, and in doing so, qualify the strength of the structure;
- **Random Vibration** to ensure primarily that the spacecraft and component boxes can withstand loads experienced during launch.

The test results can be extrapolated to predict the dynamic behavior of the Nanosat-6 design. The test planning, execution, and results are presented herein, as performed by the author with current and previous members of the Missouri S&T Satellite (M-SAT) Structures subsystem.

1.5. THESIS ORGANIZATION

Following the introduction, this work is organized into five additional parts. Section 2 opens with a brief description of shaker table vibration instrumentation and tests, followed by a review of standard vibration test practices. Section 3 is designed to familiarize the reader with the test spacecraft materials and configuration. Section 4 presents the philosophy and implementation of the vibrations tests conducted, as well as the facilities and equipment used. The test results are presented in Section 5, and finally, Section 6 discusses the lessons learned.

2. BACKGROUND

2.1. VIBRATION TEST INSTRUMENTATION

As discussed in Section 1, vibrations are generated in a device in response to some form of excitation. One method for experimental vibration involves mounting the test article on a stiff fixture and driving the fixture with a shaker table. Figure 2.1 illustrates such a set-up. An excitation signal is typically generated in accordance with the test specifications by means of a signal generator, and is applied to the test article via the shaker table after amplification and conditioning.

Sensors, such as accelerometers, are used to measure vibrations in the test object. In particular, control sensors are used to monitor whether the specified excitation is being delivered to the test object, while one or more response sensors are positioned at key locations of the object to measure its response vibrations. The sensor signals must be properly conditioned by filtering and amplification and modified, for example through modulation, demodulation, and analog-to-digital conversion, prior to recording, analyzing, and display. The purpose of the control sensor is two-fold: (1) to guarantee that the excitation is correctly applied to the test object, (2) to stabilize or limit (compress) the vibrations in the object. If the signal from the control sensor deviates from the required excitation, the controller modifies the signal to the exciter to reduce the deviation.

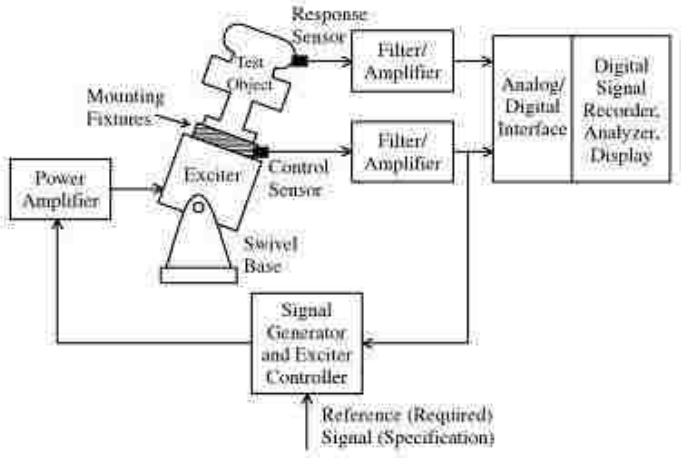

Figure 2.1. Typical Shaker Table Set-Up [16]

2.2. VIBRATION TESTS

In addition to verifying the analytical predictions for dynamic behavior, vibration tests are also useful in disclosing design or assembly flaws. For example, a loose fastener that was torqued improperly might rattle free during vibration testing. Or, vibration tests might reveal that materials or processes behave differently than designers expect.

Many of the dynamic environments described in Section 1 occur simultaneously during flight. Currently, no apparatus is available that can manifest these loads on the test structure at the same time, so they are applied according to type along each of three mutually perpendicular axes [1]. Decisions regarding which tests to conduct and which to forgo for the sake of budget or schedule limitations is rooted heavily in reliability and risk analyses [17].

2.2.1. Sine Vibration Tests. Shaker table sine vibration tests exist primarily to qualify the strength adequacy of secondary structures when subjected to a dynamic loading environment and to verify that spacecraft systems are functioning properly following other qualification tests. Additionally, they are conducted to support verification of the analytical model used in forced frequency response predictions and to determine the amplification of the excitation input from the launch vehicle interface to various components of the spacecraft -- a quality often referred to as *transmissibility*. The amplification factor, Q, is defined as the ratio of the output response to the input excitation at the resonant frequency. Transmissibility is often used to describe the effectiveness of a vibration isolation system.

Swept sinusoidal vibration tests are conducted to simulate the low-frequency sinusoidal dynamic loads. The enforced acceleration (g_{sw}) is applied in these tests by sweeping from a lower frequency limit to an upper frequency limit at a rate usually specified in octaves/minute, where an octave is double the initial frequency. Thus, from 5 Hz to 10 Hz is one octave, from 10 Hz to 20 Hz is another octave, and so forth. The sweep rate represents the velocity at which the frequency domain is scanned. For example, a swept sine vibration test might involve a sinusoid with an amplitude (A_{sw}) of 1 g, the acceleration of gravity, swept from 5 Hz to 80 Hz at a rate of four octaves/minute, which would take one minute to complete. The relationship between time *(t)* and the frequency (f_{sw}) is logarithmic.

A sine dwell test, in which the input frequency is constant, and the test proceeds for a fixed time duration or number of cycles, may also be performed. This test is designed to induce the quasi-static qualification loads. The maximum amplitude (A_{sd}) of the sinusoidal signal $\sin(2\pi f_{sd})$ must be equal to the ultimate quasi-static loads. The frequency (f_{sd}) is constrained to

$$f_{sd} \leq \frac{f_n}{3} \tag{2.1}$$

where f_n is the smallest natural frequency associated with the lowest significant vibration mode. Thus, it is difficult to apply the sine dwell test to very large structures (greater than approximately 400 pounds) because they often have low natural frequencies.

A sine burst test may also be conducted as a way to induce quasi-static qualification loads, and in doing so, verify the strength adequacy of the structure. In this case, the acceleration input signal (g_{sb}) is composed of a sinusoid

$$f(t)A_{sb}\sin(2\pi f_{sb}) \tag{2.2}$$

where A_{sb} denotes the signal amplitude, f_{sb} is the frequency, and *f(t)* represents a gradient filter. The gradient filter starts at zero and ascends to the maximum value after a number of cycles. The amplitude then remains constant for five to ten cycles and is equivalent to the quasi-static loads. Again, as with the sine dwell test, the frequency must be constrained to

$$f_{sb} \leq \frac{f_n}{3} \tag{2.3}$$

Thus, it is likewise difficult to apply sine burst tests to large structures (greater than approximately 400 pounds.) The benefit of the sine burst or sine dwell test is that it costs significantly less than a static load test [1].

2.2.2. Random Vibration Tests. Random vibration consists of many frequencies occurring simultaneously, i.e. noise. These tests are conducted primarily to test and qualify spacecraft parts, such as electronic boxes or the propulsion tank, by simulating the fairing acoustic environment and rocket engine noise. The input during a random vibration test consists of a signal between 20 Hz and 2,000 Hz, which is the typical random vibration frequency range of most launch vehicles. A test is specified by the acceleration spectral density (ASD), sometimes referred to as power spectral density (PSD), of the input acceleration, as well as by its time duration. The ASD is useful because it defines the distribution of average vibration energy with frequency. The square root of the integral of the ASD divided by frequency is defined as the root-mean-square (RMS) acceleration, g_{rms}. A sample random vibration environment test spectrum is shown in Table 2.1.

Table 2.1. Sample Random Vibration Test Environment

Axis	Frequency (Hz)	ASD Level (g^2/Hz)	Duration (s)
x, y, z	20	0.01	120
	20-50	+5.3 dB/oct	
	50-1500	0.05	
	1500-2000	-16.8 dB/oct	
	2000	0.01	
	Overall	9.24 g_{rms}	

The input ASD is measured using one or more pilot accelerometers. The signal is decoded with the aid of filters having a center frequency of f_1, f_2, f_3, ... , f_n, and an associated bandwidth of Δf_1, Δf_2, Δf_3, ... , Δf_n. The g_{rms} values being sensed by the accelerometer at each frequency can be determined with the aid of a voltmeter: $g_{rms,f1}$, $g_{rms,f2}$, and so forth. Then, the acceleration spectral density at a particular frequency, i, is given by

$$ASD = \frac{g^2_{rms,f_i}}{\Delta f_i} \tag{2.4}$$

The RMS value of the acceleration overall (along the entire frequency domain) is equal to

$$g_{rms} = \sum_{i=1}^{n} \frac{g^2_{rms,f_i}}{\Delta fi} f_i = \sum_{i=1}^{n} g^2_{rms,f_i} \tag{2.5}$$

The overall g_{rms} is useful, in that it shows how hard the shaker is working. The RMS force that the shaker must deliver is calculated using $F_{rms} = ma$, where a is the overall g_{rms} value and m represents all the masses involved, including the test articles, fixtures, and shaker armature [1].

2.2.3. Combined Vibration Tests. Since structural testing occurs at the end of a program, when schedules and budgets are often under stress, sometimes the various types of dynamic tests can be combined with considerable savings to time and budget. Combined tests also reduce the risk of damage due to handling loads. The Quick Scatterometer (QuikSCAT) satellite program made use of combined vibration testing in light of a hurried schedule. QuikSCAT replaced the original NASA Scatterometer (NSCAT), a satellite designed to record surface winds over water for several years. It experienced an unexpected failure a year after launch, and NASA built and launched its successor in less than 12 months. A quasi-static loads test, frequency identification test, random vibration test, and acoustic test were all conducted in the span of approximately one week with the spacecraft mounted to a shaker table. It was estimated that the combined testing process reduced the development schedule by at least one month when compared to a separate test campaign [19].

2.3. PURPOSE AND COMPARISON OF TESTS

In general, there are four reasons for conducting vibration tests: qualification, failure identification, workmanship, and model verification [18].

2.3.1. Qualification for Flight Environments. The primary reason for most vibration tests is to simulate the flight dynamic load environments, which would likely cause failure of many electronic components, optics, and other structures were these items not designed to survive them. Since exactly replicating the flight environment is unfeasible in most cases, vibration tests represent a simulation of the dynamic environments determined by statistical analysis of many different missions and operational conditions. The flight environments are defined using parameters of the dynamic tests that can be reasonably conducted, such as acceleration spectral density (ASD) levels.

2.3.2. Failure Identification. There have been several spacecraft that have experienced malfunctions due to dynamic environments. It is suspected that the JPL Rangers 4 and 6 failures were the result of launch vibration and that the Galileo high gain antenna's failure to open was caused by the transportation vibration environment. The problematic jitter of the original solar panels on the Hubble Space Telescope was the result of vibration generated by thermal transients. In this light, vibration tests are valuable for identifying potential problems that pose risks to mission success. For instance, at the Jet Propulsion Laboratory in Pasadena, California, vibration tests of the Cassini spacecraft uncovered an electrical grounding problem, which might otherwise have been an issue during flight.

2.3.3. Workmanship Tests. A further reason for conducting vibration tests is to identify workmanship defects, which if gone undetected, might cause damage or failure during flight. Most workmanship defects are detected at lower levels of assembly, but some interface problems can only be detected in the system level tests. For example, the equipment that caused a grounding problem in the Cassini spacecraft mentioned above underwent extensive vibration testing at the subsystem level.

2.3.4. Model Verification. Finally, vibration tests are useful in supporting verification of analytical models. This is the justification for modal tests and swept sine vibration tests that identify the natural frequencies of the structure. Natural frequencies determined during testing are compared to those predicted by the dynamic model.

2.3.5. Test Advantages and Disadvantages. As there are various types of dynamic tests with different purposes and frequency ranges of applicability, it is important to tailor a test plan to fit the needs of the program, including the reliability, schedule, and cost requirements. All dynamic tests present some risk, since the handling of a built-up spacecraft might result in damage. In general, acoustic tests are the most benign, followed by modal vibration tests, and finally shaker transient load tests. However, acoustic tests are limited to detecting workmanship defects and high frequency problems. Random vibration tests are generally safer than swept sine tests, as it is easier to limit and notch these tests. This is because it is possible to dwell at lower levels until the control system has adjusted the notches. Swept sine tests are more dangerous because the resonant frequency is sometimes passed before the control system has time to implement the notch. Shaker transient tests are the most risky because they are of very short duration and use open loop control, so over-testing may occur before there can be any chance of rectifying the situation. These tests are still popular, however, because they can replace more expensive and time-consuming static test programs.

2.3.6. Control and Limiting of Vibration Tests. While the details of the control process in vibration tests are dependent on the type of input being used (i.e. sinusoidal, random, transient), there are some common features throughout. First, most of the control is closed-loop, meaning that the input is adjusted in real time to coincide with what is desired. The exception to this is transient testing because there is generally not enough time to adjust the input. The control system may be configured to abort a transient test if the input is not as desired, but the sudden termination of a high-level test is also problematic. Sinusoidal tests are generally controlled to a peak or root-mean-square (RMS) level, and random tests are controlled to a power spectral density (PSD), also referred to as acceleration spectral density (ASD), level. In both cases there is some preset tolerance and some threshold for automatic shut down.

In addition to closed-loop control, it is also common practice in spacecraft vibration testing to have limit channels, which are used to modify the control if these channels start to exceed their specified limits. In both sinusoidal and random tests, these limits may be a function of frequency, and the input may be reduced, "notched," at frequencies where the limit is exceeded. These are typically the frequencies at which the test item has resonances, which are structural characteristics that form its unique dynamic signature. Even a seemingly solid structure will exhibit significant deflections when its resonant frequencies are excited, so it is important to limit the input at structural resonances to avoid over-testing beyond the design limits. This may be accomplished through imposing limits on acceleration or forces. Several response accelerometers may be placed at key points on the test article and linked to the control algorithm to notch input levels to the shaker. This is the most common means of response limiting, but the advent of compact and stiff tri-axial force gages has made limiting the forces between the shaker and the test item increasingly popular.

There is always a compromise between the complexity of the test set-up and operations, and the number of safeguards and limits to wisely implement. This balance is based on the sophistication of the test hardware, the test equipment, and operators. If too many limit channels are used, the vibration controller may be slow to update the input and sense over-testing.

2.4. TEST PLAN DEVELOPMENT AND IMPLEMENTATION

The test plan generally refers to the plan for testing a specific hardware item, such as the flight spacecraft. The test implementation, on the other hand, refers to the test procedure, or the detailed steps of conducting the test [18].

2.4.1. Requirements Definition. Requirements come in many forms, and may flow down from external organizations or the functional objectives of the mission. While some requirements may be difficult to change, and others may be negotiable, they should always be scrutinized to ensure their applicability to the test item under consideration. In the past, each institution often had its own set of requirements that were contained in various test standards, and compliance with the standards was mandatory. Today, there tends to be much more flexibility and willingness to allow each project to tailor the

testing requirements to its specific needs. In the case of commercial spacecraft, however, the insurers often set the test requirements.

A set of baseline requirements should always be defined at the beginning of each dynamic test program. Allowing requirements to evolve as a result of the abandonment of certain mission objectives will usually yield a non-optimal program and wasted resources. The baseline program should include sufficient testing to satisfy the requirements for qualification of the ability of the system to withstand flight dynamic loads, workmanship testing, and verification of models used in structural response predictions. For example, most programs would require a test to verify the survivability of the structure against acoustic loads; most would include some type of modal test to determine the natural frequencies of the structure, and many programs would implement a vibration test with the spacecraft mounted on a shaker table. Of course, cost and schedule, the heritage of the spacecraft, and the severity of the flight environments will factor into the number and type of tests needed.

There is also a logical requirement that subsequent tests should be more benign than the ones preceding them, so that the early tests should prove the survivability of the spacecraft. For example, tests conducted on the flight structure are usually performed at lower levels than those conducted earlier on a qualification structure. Similarly, the tests conducted at higher levels of assembly are usually less severe than those conducted on the subsystem units or components.

2.4.2. Pre-Test Analysis. One of the most important aspects of test planning is the pre-test analysis, because it offers insight into the expected response of the spacecraft to a particular input, as well as the knowledge to deal with it in advance of the test. This allows the actual test process to go much faster and permits the attention during the test to focus on new problems that could not be anticipated. The most common type of pre-test analysis consists of a simulation of the actual dynamic test using numerical models. For vibration tests, a finite element model (FEM) is often used.

2.4.3. Preparation of the Written Test Plan. The test plan is usually prepared well in advance of the actual test. Its purpose is to present a description of the test for review and editing and to facilitate coordination of the many activities that must take place for the test item and test facility to be ready and the test to be successful. The written test plan covers topics such as:

- Test hardware definition (i.e. prototype or protoflight);
- Description of the test facility and equipment;
- Definition of the test fixture;
- Definition of the instrumentation (i.e. accelerometers, force gages, strain gages);
- Test specification and limits;
- Description of the test runs and intermediate data analysis;
- Naming of the test director and other key personnel and the defining of their responsibilities;
- Determination of the safety and cleanliness requirements and precautions.

2.4.4. Hardware Definition. The first topic discussed in both the test program and the test plan is usually the test item. Its extent and configuration are defined, such as whether it will consist of prototype or protoflight hardware, contain mass simulators or actual components, or possess a combination of these. Usually the test plan will include drawings, solid model pictures, or photos of the test hardware showing the major components and interfaces. The coordinate system(s) and interfaces should be well-defined.

2.4.5. Facilities and Personnel. Test facilities need to be identified and described in detail in the test plan. The facility must have the capability to safely implement the test requirements, while meeting cleanliness and handling specifications. It is also a good idea to inquire as to the recent use of the facility in conducting corresponding tests on similar hardware and the experience of the test operators. Good communication is essential with the facility personnel, so that the typical methods for conducting tests can be respected, and a good working relationship can be established.

2.4.6. Fixtures. Shaker table vibration tests usually require that the test item be mounted on some type of fixture, which is often specific to the item itself. It is important to communicate with the test facility personnel to discuss the fixture configuration and its interfaces with the shaker table. The fixture should be fit-checked with the test item, and if possible, the shaker table and other ground support equipment in advance of the test.

2.4.7. Instrumentation. It is often necessary, or at least advantageous, to install some of the instrumentation before the test. The most common form of instrumentation for structural tests is accelerometers, which come in a variety of sizes, sensitivities, and frequency ranges, depending on the application. Other types of instrumentation include force gages, strain gages, and occasionally temperature sensors. Often on system level tests, many of the interior instrumentation locations are accessible only at specific points in the assembly of the test items. In these cases, it is important for the test personnel to communicate closely with integration engineers to ensure that instrumentation is placed in the proper locations. Sometimes these instruments are removed post-test if the item is partially disassembled, or sometimes the cables are cut and the instruments actually fly.

2.4.8. Test Options and Test Sequence. There are various options for conducting dynamic tests. For example, acoustic tests might be conducted in a reverberant chamber, with speakers in a high bay, or in the case of lower budget programs, random vibration tests conducted on a shaker table can be substituted to simulate the acoustic loading environment. A modal survey might be conducted with the spacecraft mounted on an inertial mass or on a shaker table, or suspended freely. Other test options involve the decision to use protoflight hardware or dedicated test structures, known as development test models. There is also the option of combining dynamic tests to save time and reduce costs.

The significance of following a certain test order is recognized and often specified in the requirements from a launch vehicle provider or other external institution. The number of test runs depends on the complexity of the test item, the number of test configurations and axes, and the problems encountered during the tests. It is common practice to begin with a low-level signature or health monitoring run in each configuration, which is normally repeated after the full-level testing. Normally, a number of low-level tests are conducted, with some data analysis and review between each run,

before moving on to the full-level test. Sometimes the lowest level run is conducted with and without force limiting. It is best if all of the limits scale down with the inputs in lower-level runs, so that any problems may be identified and corrected by adjusting the limits before the full-level test. Typically, lower-level runs are conducted for a shorter time interval, with the only requirement being the time necessary to acquire valid data. Thirty seconds is typical for lower-level runs. If the test structure contains electronic, mechanical, or optical equipment, it is also a good idea to conduct functionality or "aliveness" tests between configuration changes.

2.4.9. Equipment Operation and Control. Over-testing failures are not uncommon, so it is important that proper control of the vibration test be maintained at all times. It is essential to ensure that the shaker table does not malfunction and that the test personnel do not make any errors in operating the equipment. A good practice is to limit the working hours to a standard day when possible, and to avoid the most dangerous, high-level tests late at night or first thing in the morning. The input to the test should be reviewed before and after each run, to ensure that it is correct and within test tolerances.

A pretest should be conducted as close in advance to the actual test as possible. The purpose of the pretest is to exercise the equipment before the test item is installed to ensure that it is functioning properly and to serve as a "dry run" for test personnel. This pretest should include any fixtures and a mass simulator if the weight of the test item is appreciable (greater than 50% of the shaker capability). During the pretest, the control accelerometers should be installed in the same positions as for the actual test.

2.5. RESULTS INTERPRETATION

At the completion of a systems dynamics test, it is always good practice to reflect on the lessons learned, such as:

- Were the test inputs correct?
- Was there any under- or over-testing?
- How could the procedure be improved for future tests?
- Were there any structural, electrical, or functional failures of the test item?
- Was there any significant wear or deterioration, which should be remedied or

taken into account during future testing? How should these results be documented?

- Are the test data consistent with model predictions, and if not, why not?
- Were there any insights that can be applied to tests in the same or other programs?

2.5.1. Structural Integrity. A structural failure is the most significant event that can happen during a dynamics test. Sometimes a structural failure is accompanied by a noise or visual observation, but often, failures are observed only when the test item no longer operates properly in a post-test mechanical functionality test, or when the test item is disassembled and loose parts or damage is discovered. The before-and-after test traces observed in the vibration signature tests are seldom identical, so it is usually difficult to make the decision to stop testing or to disassemble the test item to look for damage on the basis of signature changes. Sometimes, a small change is cleverly recognized as the indicator of a structural failure, while other times the cause of a frequency shift, or in some cases even the complete disappearance of a frequency peak, is never found. The decision of whether to stop or proceed with testing after a signature change usually requires a caucus of the technical specialists and the project personnel. If no damage has been observed in a visual inspection, the test item performs normally in a mechanical functionality test, and there are no anomalies in signature tests, it may be concluded that the test item maintained its structural integrity. However, the item may still have undergone some wear, such as the joints may have loosened or the structure may have used up some of its fatigue life through the growth of an undetectable fatigue crack.

2.5.2. Post-Test Analysis. There are several reasons to conduct post-test analysis, such as: to tune the analytical model with the test data; to understand why a structural failure occurred; to predict the dynamic behavior of the test item after a design change; or to extrapolate the dynamic response of the test item to a different test or flight environment. The merging of test and analysis in order to extrapolate dynamic test data to predict the response of a modified or new test item in a dynamics test is the most challenging type of post-test analysis.

2.5.3. Design Iterations and Retests. The first step in dealing with a structural failure is to determine its root cause, which is very important but often difficult. Without knowledge of the root problem, however, it is impossible to determine how to correct the problem or whether it has been fixed. Sometimes a failure is caused by a cascade of events: a bolt may back out and excessive motion may result in stresses exceeding the design limit. Other times, it is simply a case of the design margins of a number of parts in a mechanism being too low. A common mistake is the use of too low a multiplier on the root mean square value in a random vibration test, which is used to estimate the maximum stress that will occur during the test. Although the shaker table random vibration inputs are clipped at three sigma, responses can exhibit peaks with higher values of sigma.

In some cases it is recommended that the suspected cause of failure be verified through retesting the old design with additional instrumentation. If the failure is determined to be associated with a design problem, the design should be changed so that all of the relevant design margins are significantly increased. Finally, it will be necessary to test the new design to verify that the problem has been resolved.

2.5.4. Verification and Validation. Verification testing is usually conducted to check or corroborate an analytical model and/or to assure that the design meets the specified requirements. Random vibration or acoustic tests are used to verify the workmanship of the test item. Or, it might be necessary to verify that the spacecraft has a fundamental resonance above 50 Hz. Test data might be used to improve the finite element model so that it may be used with confidence to predict the response behavior of the spacecraft to a different environment, for which no test is planned. According to NASA standard 5002, *Load Analyses of Spacecraft and Payloads*, agreement between the analytical and experimentally found natural frequencies should be within 5 percent for the significant modes.

Validation testing is more fundamental than verification testing. Validation implies more of an end-to-end check of the whole design and fabrication process including the starting points and assumptions. System qualification tests for a flight dynamic environment such as random vibration or acoustics are examples of validation tests.

3. TEST STRUCTURE OVERVIEW

Satellite design begins with a top-level mission requirement, followed by several systems engineering studies to determine factors such as power and mass budgets, the best trajectories and orbits for mission objectives, and how much propellant will be needed. In addition to the mission constraints, size and mass restrictions are essential for reducing the costs associated with launching a satellite. Limiting the spacecraft volume, however, results in a complex series of tradeoffs between conflicting elements in the design.

3.1. M-SAT MISSION SUMMARY

Students working in the Space Systems Engineering Laboratory at Missouri S&T (the M-SAT team) are working toward the design, fabrication, and test of a protoflight spacecraft. At the time of this research, the spacecraft consisted of two microsatellite structures, Missouri Rolla Satellite (MR SAT) and Missouri Rolla Secondary Satellite (MRS SAT), which were designed to investigate distributed space systems technologies, while performing an autonomous formation flight mission. Upon reaching their desired orbit, MR SAT and MRS SAT were designed to decouple, and MR SAT would enter a chase mode to establish a close-formation flight with MRS SAT. Figure 3.1 shows the satellites as they would have appeared in formation.

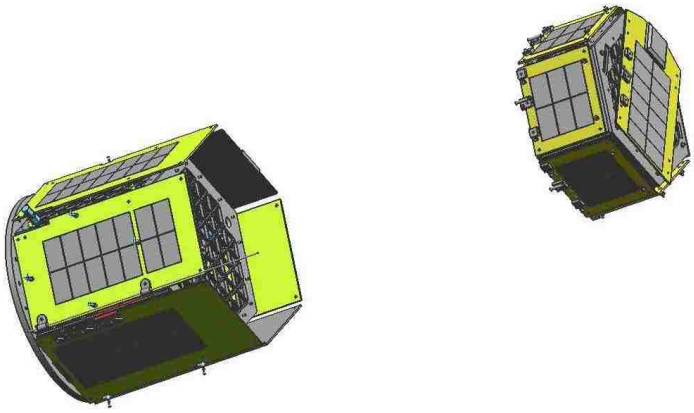

Figure 3.1. MR SAT and MRS SAT In-Flight Formation

The use of "fractioned" spacecraft offers a variety of advantages over a traditional satellite, in which all hardware is enclosed in a single structure. Multiple satellite units allow for mission-essential equipment to be spread among several spacecraft, greatly reducing the chances of a critical failure.

3.2. STRUCTURAL DESIGN CONSTRAINTS

Once the M-SAT mission objectives were determined, a list of design requirements and constraints was prepared. Some of these requirements and constraints flowed down from the University Nanosat Program (UNP), while others were the result of mission objectives. The M-SAT constraints are summarized below in Table 3.1.

Table 3.1. M-SAT Mission Constraints

System	Description	Requirements		
		Minimum	**Goal**	**Achieved**
Orbit	Altitude (km) Eccentricity Inclination	190 Approx. zero 39^{o}	700 0 56^{o} or higher	Determined by launch vehicle
Operational Life	Total time in orbit	2 weeks	2 years	TBD
Structure	Shape Length (cm) Width (cm) Diameter (cm) Height (cm) Mass (kg)	Right cylinder N/A N/A ≤ 60 ≤ 50 ≤ 50	To meet the minimum requirements for the UNP	Hexagonal Prism N/A N/A 43.4 cm 49 cm 29.39 kg
Communication	Satellite to ground Satellite to satellite	Data rate adequate for telemetry Custom inter-satellite comm. system	Multifunctional RF transceiver Radio using Bluetooth technology	Purchased receiver and transmitter Bluetooth hardware purchased
Power	Electrical power throughout mission	One orbit, primary batteries	Longer mission, solar cells and batteries with power regulation	Solar panels; batteries; power regulation board

The University Nanosat Program placed several constraints on the satellite structure, which included:

- Total mass of less than 50 kg
- Must fit within an allowable static envelope with linear dimensions of 60 cm in width and length, and a height of 50 cm
- The center of gravity (CG) of the system shall be less than 0.635 cm from the centerline and less than 30.48 cm above the satellite interface plane (SIP) (+Z-axis)
- Must be capable of withstanding a limit load of 20-g's in the X-, Y-, and Z-directions with a factor of safety of 2.0 for yield and 2.6 for ultimate
- Possess a fundamental frequency above 100 Hz given a fixed-base condition at the SIP

The 100 Hz frequency condition is considered a "hard requirement," while the mass of the spacecraft is the associated "soft requirement." It should be noted that designing strictly to the required factors of safety should get the spacecraft close to a fundamental frequency of 100 Hz. However, if the stiffness requirement is used as the primary driver in design, static load analysis ought to show that the loading factors of safety will already be met.

3.3. M-SAT TEST STRUCTURE

3.3.1. Primary Structure. The primary structure essentially acts as the backbone of the spacecraft, mechanically supporting the systems and instruments and ensuring components remain aligned during flight. A cylindrical or spherical design will maximize the available volume, while a cube-like shape allows for the simplest assembly and attachment of components. After trade studies were performed by the M-SAT team, a hexagonal shape was determined to be the best compromise. The structures of MR and MRS SAT are shown in Figures 3.2 and 3.3, respectively.

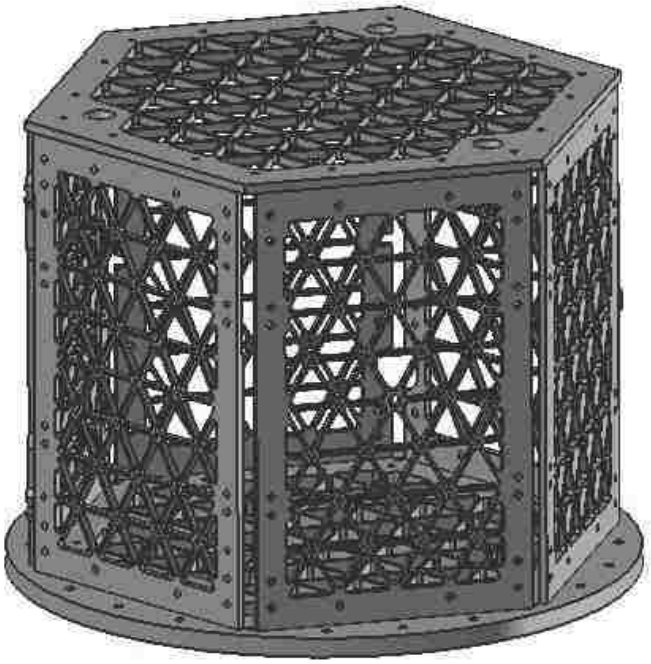

Figure 3.2. MR SAT Structure

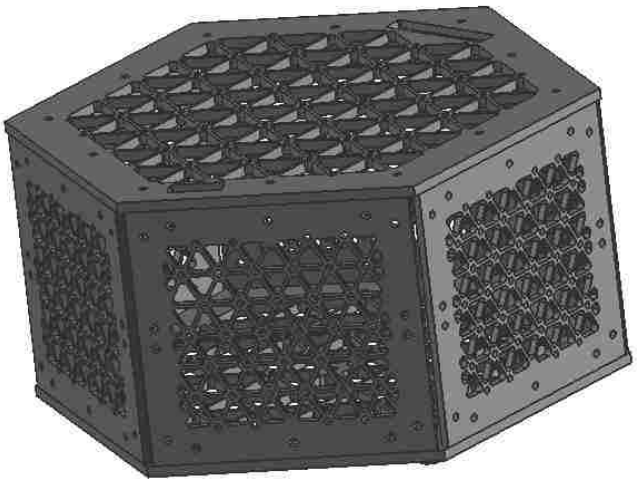

Figure 3.3. MRS SAT Structure

The M-SAT primary structure is constructed from 6061-T6 aluminum alloy, chosen for its high strength-to-weight ratio, its workability, resistance to stress corrosion and cracking, and its standard use in aerospace applications, making it inexpensive and

widely available. All structural components were machined at Missouri S&T. The top, bottom, and side panels of MR and MRS SAT were modeled in an isogrid pattern, as this reduces the structural mass while maintaining adequate strength and stiffness. The side panels are shown in Figures 3.4 and 3.5. Furthermore, the nodes of the isogrid panels serve as attachment points for secondary components.

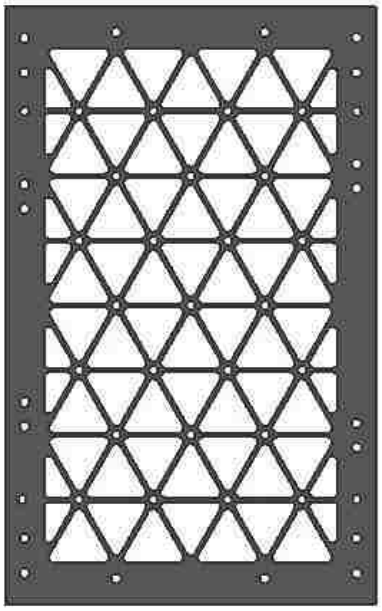

Figure 3.4. MR SAT Isogrid Panel

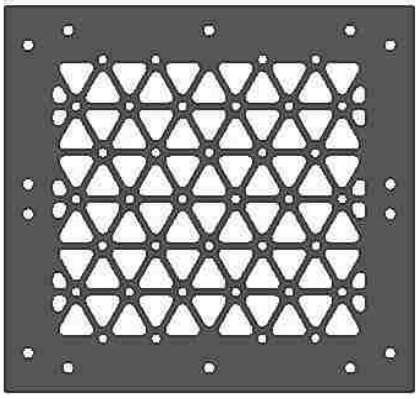

Figure 3.5. MRS SAT Isogrid Panel

For both MR and MRS SAT, brackets were designed at a 120-degree angle for attaching the side panels to each other, and at a 90-degree angle for connecting the side panels to the top and bottom plates. Corner brackets were machined and positioned at every corner. The bracket connections are shown for MR SAT in Figure 3.6. The 120-degree brackets were designed to attach on the outside for ease of assembly. All other brackets used to connect the primary structure are fastened from the satellites' interiors.

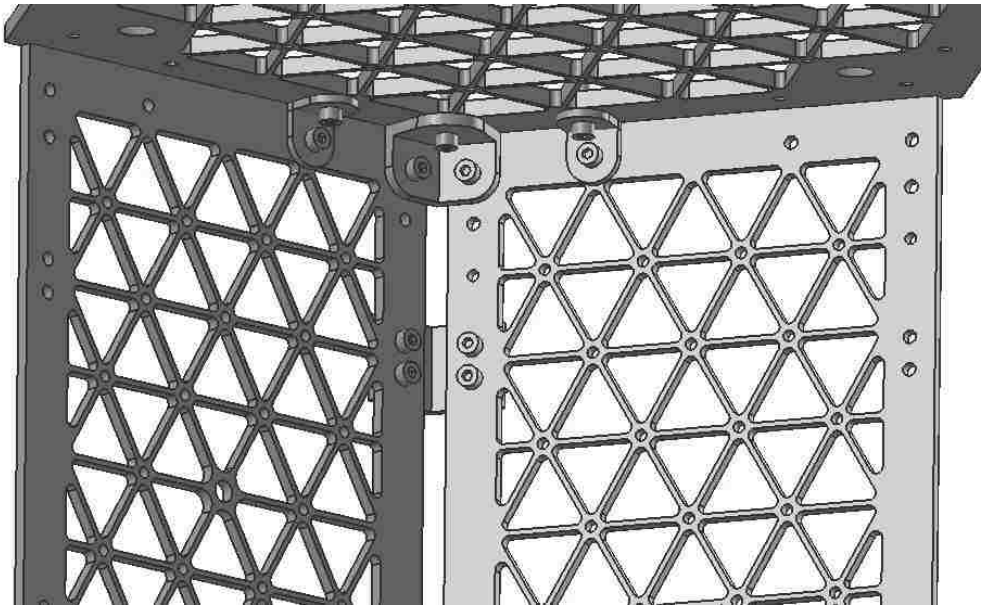

Figure 3.6. MR SAT Brackets

Primary structural components were attached using #10-24 stainless steel socket head cap screws and lock nuts. Components were attached to the isogrid panels using #8-32 stainless steel socket head cap screws and lock nuts. These fasteners were chosen based on recommendations by the Air Force Research Laboratory.

3.3.2. Spacecraft Components. There are nine subsystems with components to be integrated into the M-SAT isogrid structure. Table 3.2 shows a comprehensive list of those components at the time of this research. Components listed in gray were replaced with mass simulators during vibration testing. Those listed in red had not yet been manufactured, or were not included in the test assembly.

Table 3.2. M-SAT Component List by Subsystem

Subsystem	*Component*
Structure	QwkNut
	Bolt Retractor
	Zip-ties
	Component boxes
	Bolts/nuts/spacers
	Helicoils
	Honeycomb Al panels
	Magnetometer adapter plates
	Transmitter adapter plate
	Coil mount assemblies
ADAC	Magnetometers
	Coils
Orbit	GPS receivers
	GPS antennas
	GPS interface board
Communication	Transmitter
	Receiver
	Bluetooth transceivers
	Bluetooth mounting board
	Bluetooth antennas
	Transmitter antenna
	Receiver antenna
	Cables
	Modem
	Communications power board
Power	Solar cells
	Battery Box
	Batteries

Table 3.2. M-SAT Component List by Subsystem (Cont.)

Subsystem (cont.)	*Component (cont.)*
C&DH	Viper boards
	Power boards/charge controllers
	Propulsion board
	Magnetic coils boards
	Magnetometer boards
	Thermal boards
	Connectors
	Wire
	Acrom Viper computer
Thermal	Thermal sensors
	Coatings
Propulsion	Tank and tank mounts
	Propellant
	Transducers
	Regulator
	Valves
	Nozzles
	Tubing
	Heaters
	Fill/Drain valve
	Connectors
GSE	Lift tabs
	Lightband release mechanism bolts

3.4. TEST SPACECRAFT CONFIGURATION

3.4.1. Dimensions. The overall dimensions of the satellite test structure are provided below in Figures 3.7 through 3.9. Dimensions are given in both millimeters and [inches].

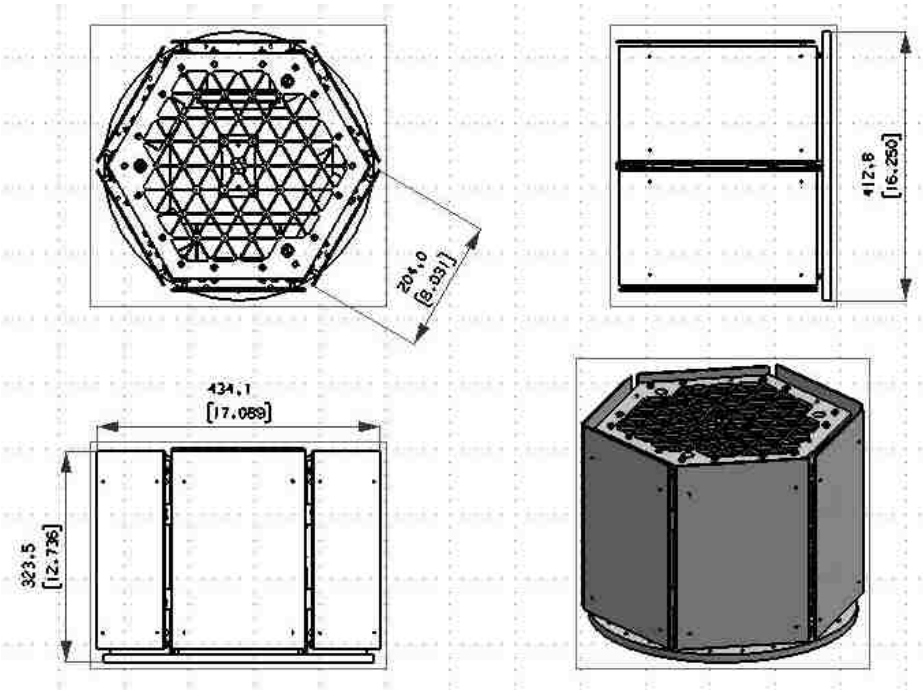

Figure 3.7. MR SAT Overall Dimensions

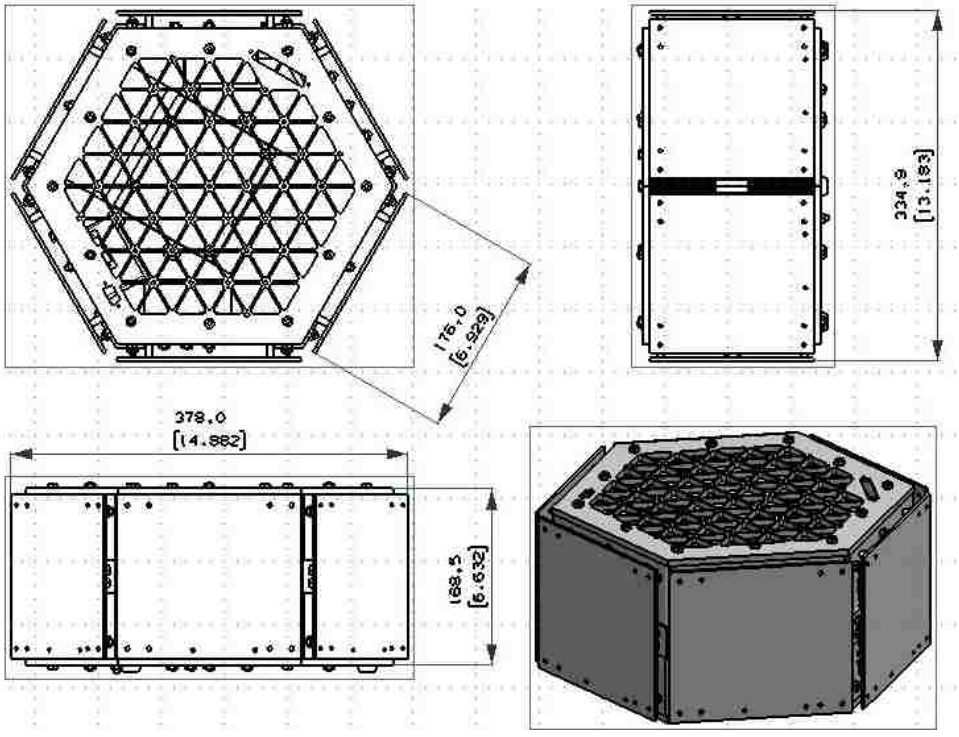

Figure 3.8. MRS SAT Overall Dimensions

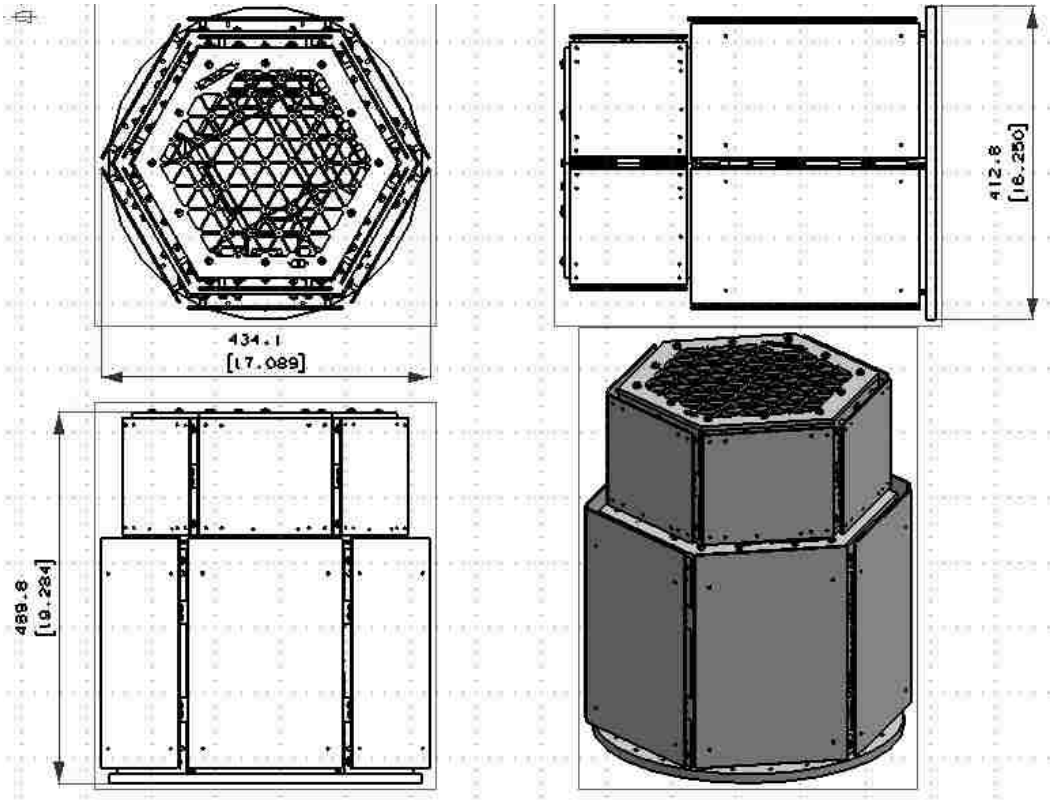

Figure 3.9. Docked Configuration Overall Dimensions

3.4.2. Mass Properties. The test structure mass properties are provided in Tables 3.3 through 3.5. Figure 3.10 shows the center of mass reference frame with the bottom plate of MR SAT defining the X-Y plane, and the Z-axis aligned with the center of the spacecraft.

Table 3.3. MR SAT Mass Properties

		Center of Mass (mm from center)		Centroidal Moments of Inertia (kg mm^2)	
Area	32,817.46 cm^2	$\overline{x_c}$	-2.20	I_{xx}	454,558
Volume	6,326.729 cm^3	$\overline{y_c}$	15.77	I_{yy}	410,816
Mass	19.63 kg	$\overline{z_c}$	130.50	I_{xx}	458,117

Table 3.4. MRS SAT Mass Properties

		Center of Mass (mm from center)		Centroidal Moments of Inertia (kg mm^2)	
Area	17,900.55 cm^2	$\overline{x_c}$	11.75	I_{xx}	112,099
Volume	3,072.413 cm^3	$\overline{y_c}$	-9.38	I_{yy}	124,197
Mass	9.76 kg	$\overline{z_c}$	83.55	I_{xx}	182,801

Table 3.5. Docked Configuration Mass Properties

		Center of Mass (mm from center)		Centroidal Moments of Inertia (kg mm^2)	
Area	50, 718.01 cm^2	$\overline{x_c}$	3.19	I_{xx}	1,058,789
Volume	9,399.143 cm^3	$\overline{y_c}$	12.57	I_{yy}	1,026,831
Mass	29.39 kg	$\overline{z_c}$	221.64	I_{xx}	643,240

Figure 3.10. Spacecraft Reference Frame

3.4.3. Satellite Interfaces. The bottom plate of MR SAT is circular, in order to accommodate the launch vehicle separation mechanism. There are 24 bolted connections for rigid attachment. Due to the separation mechanism's design characteristics, there are strict requirements on the bottom panel design of MR SAT that include a stay-out zone for any hardware and a flatness requirement.

There is also a system-level requirement that the two satellites remain in a docked configuration until the separation mode of the mission. At the time of this research, the satellites are held together by one 1/4"-28 bolt secured at up to 3,000 ft-lb torque. It is desirable for the separation mechanism between the satellites to be redundant, or at least highly reliable. A trade study resulted in the selection of the QwkNut 3K non-explosive actuator (NEA) device provided by Starsys. This design involved the use of one QwkNut mechanism attached to the top panel of MR SAT, and a Bolt Retractor mechanism attached to the bottom panel of MRS SAT to prevent the connection bolt from being discharged into MRS SAT following release of the QwkNut device.

The interface between MR and MRS SAT requires that the satellites be held stable to prevent twisting or compressing during launch. To circumvent the need for a flatness requirement on the bottom panel of MRS SAT and the top panel of MR SAT, the satellites only make contact at three points that are separated by 120 degrees. This also serves as a cup/cone arrangement to prevent twisting of the satellites with respect to each other. The satellite interface is shown in Figure 3.11.

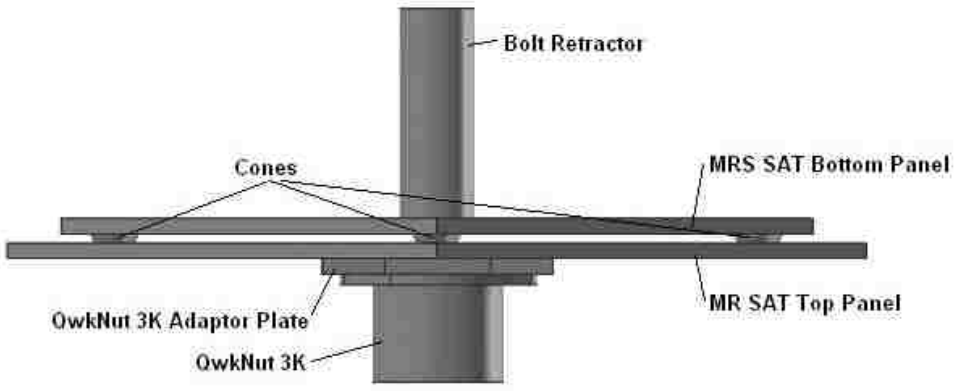

Figure 3.11. MR and MRS SAT Mechanical Interface

3.4.4. Satellite Configurations. The orientation and placement of all of the components in the M-SAT structure was an iterative design process. Most components are required to be housed in aluminum boxes, which must be designed to attach at the nodes of the isogrid pattern on the primary structure. The uniqueness of the components and the different isogrid patterns of MR and MRS SAT led to each box being distinct in its design. Figures 3.12 through 3.15 show the configuration of the satellites, including "flowered" views displaying the component placement.

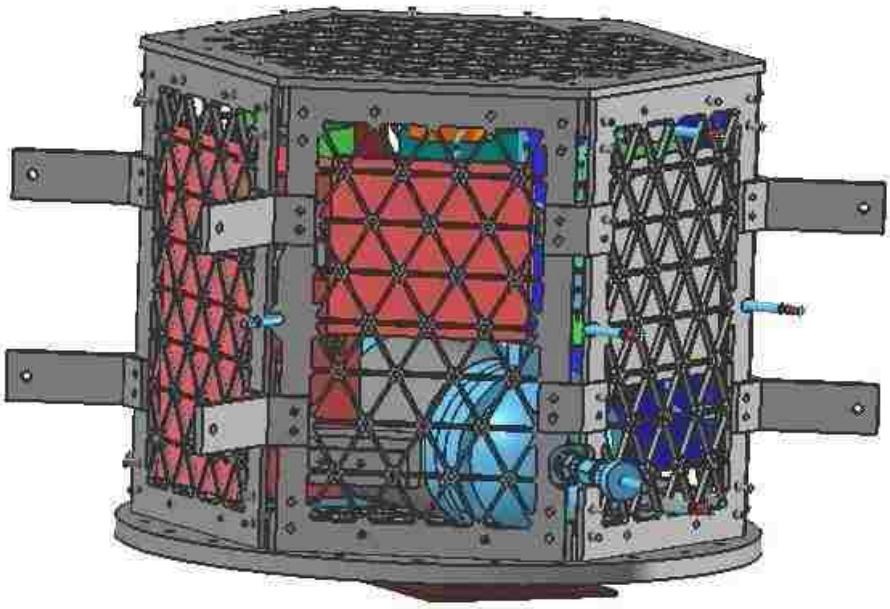

Figure 3.12. MR SAT Configuration

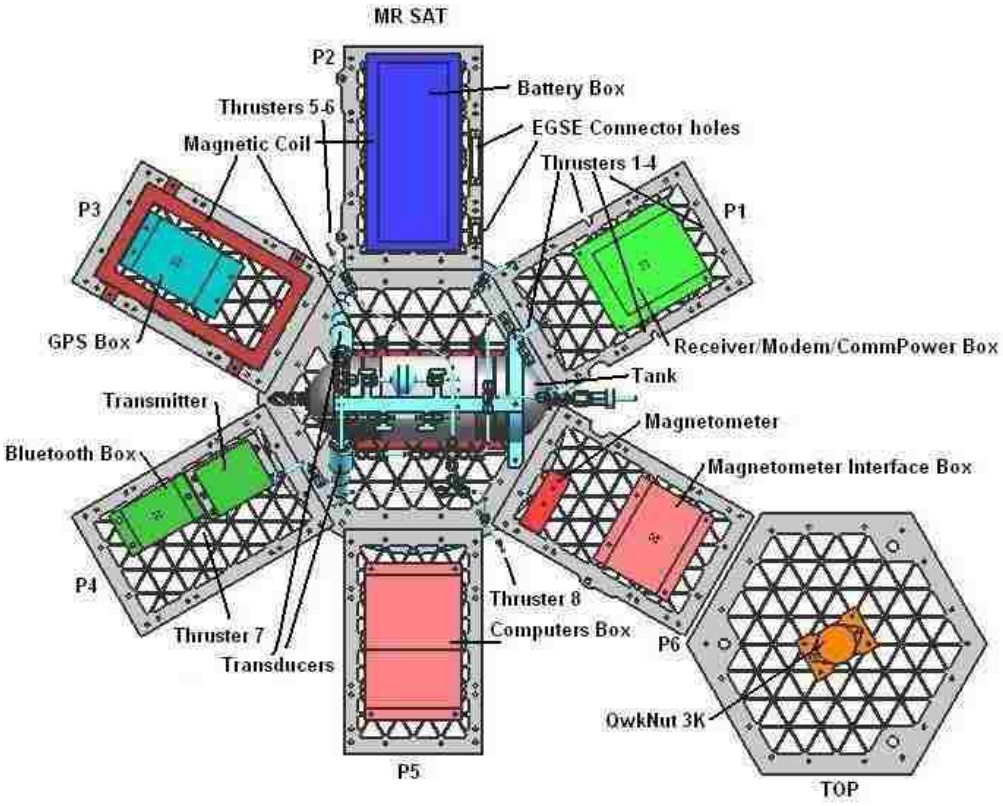

Figure 3.13. MR SAT Flowered View

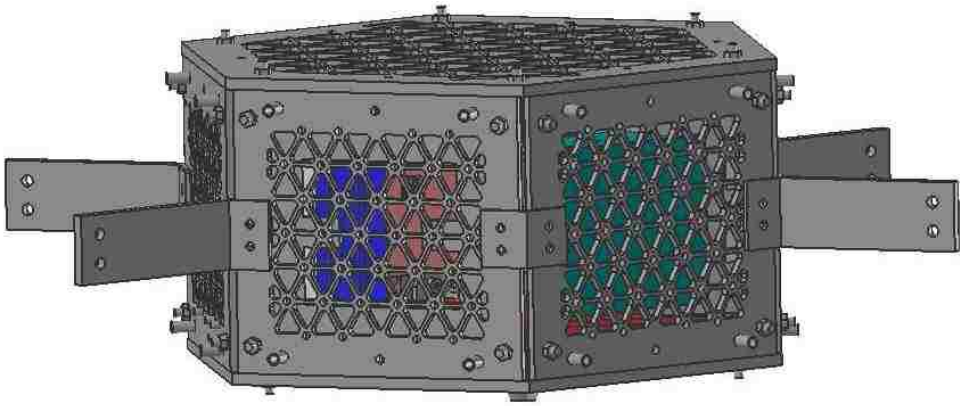

Figure 3.14. MRS SAT Configuration

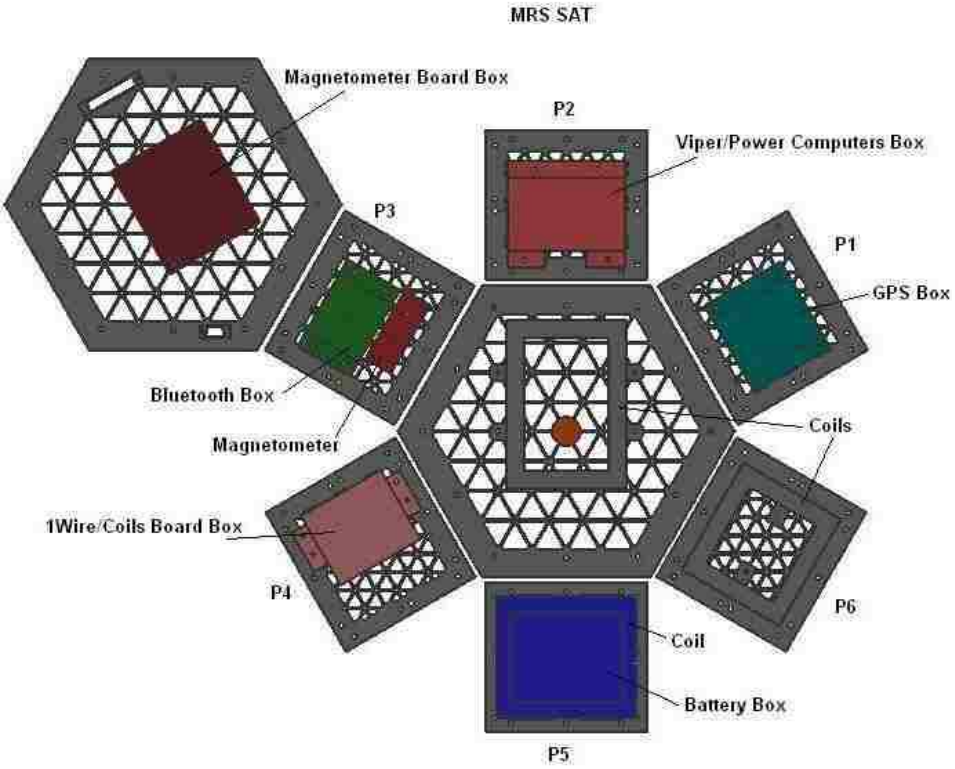

Figure 3.15. MRS SAT Flowered View

4. TEST PLAN AND IMPLEMENTATION

4.1. TEST SPECIFICATIONS

4.1.1. Sine Sweep. To meet the Nanosat-6 structural requirements, the spacecraft must be engineered with a fixed-base natural frequency greater than 100 Hz at the satellite interface plane, in order to ensure an overall payload stiffness greater than 50 Hz after integration with the launch vehicle. The university was required to demonstrate by analysis and test that the M-SAT spacecraft could meet this requirement.

Acceptable tests for verifying natural frequencies include modal survey or swept sine vibration. M-SAT performed a swept sine vibration test on the satellites from 20 Hz to 2,000 Hz at 0.25 g. The sweep frequency range and acceleration were set forth by the Air Force Research Laboratory (AFRL) in the University Nanosat Program (UNP) Nanosat-6 User's Guide [20].

4.1.2. Sine Burst. As mentioned in Section 2.1.1 above, a sine burst test may be conducted as a way to induce quasi-static qualification loads, and in doing so, verify the strength adequacy of the structure. A sine burst test was performed at a level 1.2 times limit loads at a frequency that was one-third the lowest natural frequency of the test article. The lowest natural frequency was determined analytically using finite element analysis and verified experimentally via a swept sine test. During the sine burst test, no detrimental permanent deformation or ultimate failures should occur.

4.1.3. Random Vibration. The integrated satellite system must be able to withstand the launch vehicle vibroacoustic environment without failure. The random vibration environment test spectrum is presented below in Figure 4.1 and Table 4.1, as specified in the Nanosat-6 User's Guide.

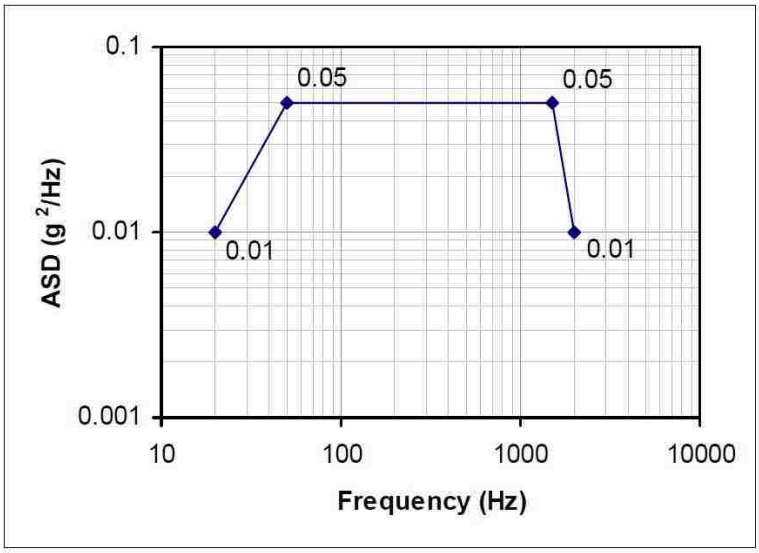

Figure 4.1. Nanosat Random Vibration Test Levels

Table 4.1. Nanosat-6 Random Vibration Spectrum Test Levels

Axis	Frequency (Hz)	ASD Level (g^2/Hz)	Duration (s)
x, y, z	20	0.01	120
	20-50	+5.3 dB/oct	
	50-1500	0.05	
	1500-2000	-16.8 dB/oct	
	2000	0.01	
	Overall	9.24 g_{rms}	

4.2. TEST SEQUENCE

As mentioned in Section 2.4, it is a common requirement that vibration tests be performed in a certain sequence, such that subsequent tests should be more benign than the ones preceding them. In this way, the early tests should prove the survivability of the spacecraft. The Nanosat-6 User's Guide states that universities are required to verify by experimentation that the spacecraft has a fixed-base fundamental frequency greater than 100 Hz, which the M-SAT team accomplished via a swept sine test. UNP does not

require the university to perform a sine burst or random vibration test, as these will be conducted on the flight-configured winning spacecraft by AFRL personnel. However, the M-SAT team chose to conduct these tests, as well, to validate the space worthiness of the satellites and detect any issues that might affect the spacecraft during flight. For reference purposes, the full environmental test flow to be performed on the winning Nanosat-6 spacecraft by AFRL is shown in Figure 4.2.

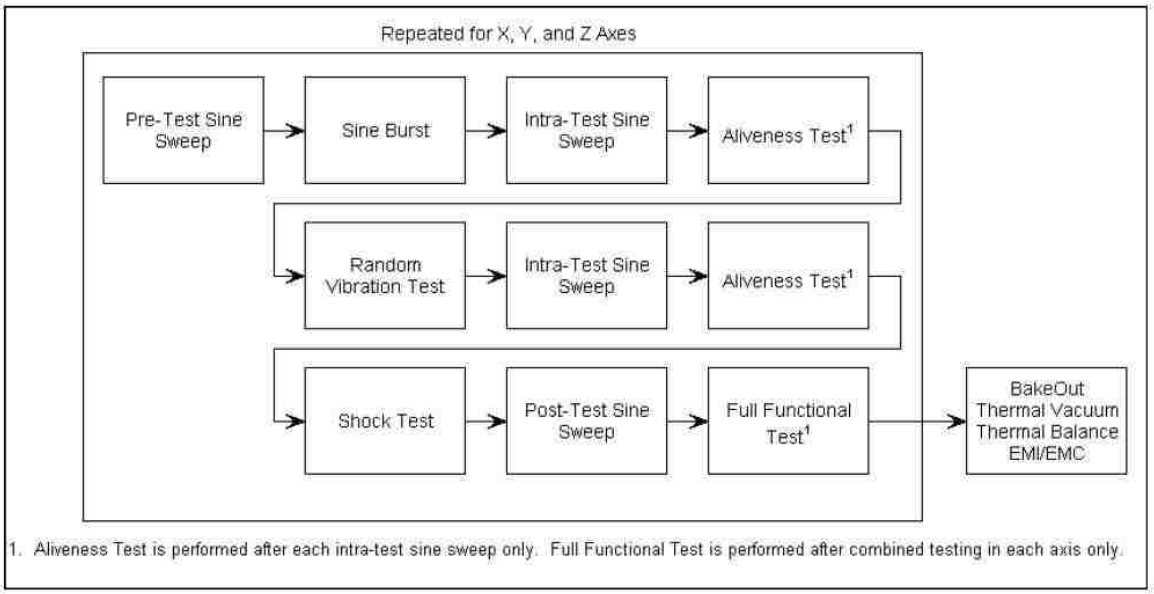

Figure 4.2. AFRL Environmental Test Flow [20]

In keeping with the AFRL test flow, the M-SAT team performed an initial swept sine test to verify that the fundamental frequency of the spacecraft corresponded to the team's finite element analysis. A sine burst test was subsequently performed, followed by an intermediate swept sine test. The vibration signature of the second swept sine test was compared to the initial vibration signature to assist in determining whether any structural damage occurred during the sine burst test. As no flight electronics were incorporated into the test structure, an aliveness test was inapplicable. Finally, a random vibration test was conducted, followed by another swept sine test to again obtain the vibration signature. The M-SAT vibration test plan stated that the swept sine, sine burst, and

random vibration tests be performed on MR SAT, MRS SAT, and the spacecraft docked configuration, independently, in three mutually perpendicular axes.

4.3. EQUIPMENT AND HARDWARE

The M-SAT vibration tests were conducted on an electrodynamic shaker at the Caterpillar facility in Peoria, Illinois, under the direction of Caterpillar test personnel. The shaker (model V860-610) was manufactured by Ling Dynamic Systems, as was the power amplifier to the shaker (model SPA-56K), which has a 24 kVA output. The shaker controller (model VR8500) was manufactured by the Vibration Research Corporation in Grand Rapids, Michigan.

The satellites are shown mounted to the shaker table in Figure 4.3. This configuration is used to perform vibration tests in the Z-direction, as denoted by the spacecraft reference frame in Figure 3.10. The shaker table must be rotated 90 degrees to perform vibration tests in the X- and Y-directions. A Caterpillar test operator is shown using a crane to rotate the shaker table in Figure 4.4.

Figure 4.3. MR SAT (Left) and MRS SAT Shown Mounted to the Shaker Table

Figure 4.4. Rotating the Shaker Table for X- and Y-Axis Tests

Electrodynamic shakers generate motion using the operating principles of an electric motor. Specifically, the excitation force is produced when a variable excitation signal is passed through a moving coil placed in a magnetic field. A steady magnetic field is created by a stationary electromagnet that consists of field coils wound on a ferromagnetic base. The shaker head, which is supported on a flexure mount, is also wound with a coil. When the electrical excitation signal is passed through this drive coil, the shaker head is set in motion. Figure 4.5 shows the components of a commercial electrodynamic shaker.

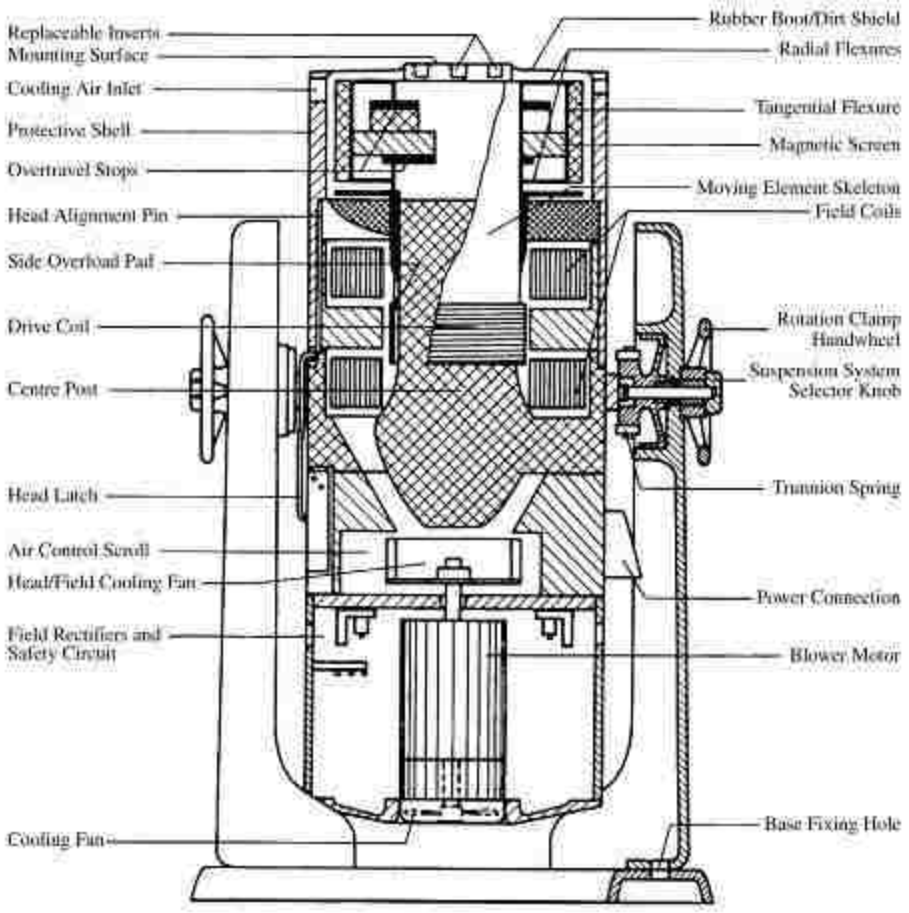

Figure 4.5. Commercial Electrodynamic Shaker [16]

Custom mounting fixtures for MR and MRS SAT, illustrated in Figures 4.6 and 4.7, were designed by the M-SAT Structures subsystem. It was important that the team communicate with the Caterpillar test facility personnel to discuss the fixture configuration and its interfaces with the shaker table. After the designs for both fixtures were approved, a work order was submitted to the Machine Shop at Missouri S&T for their manufacture. The mounting fixture for MR SAT was designed with 24 bolt locations for the rigid attachment of MR SAT. This design best replicated integration with the launch vehicle separation mechanism. The MRS SAT mounting fixture was designed to replicate the interface with the top plate of MR SAT shown in Figure 3.11.

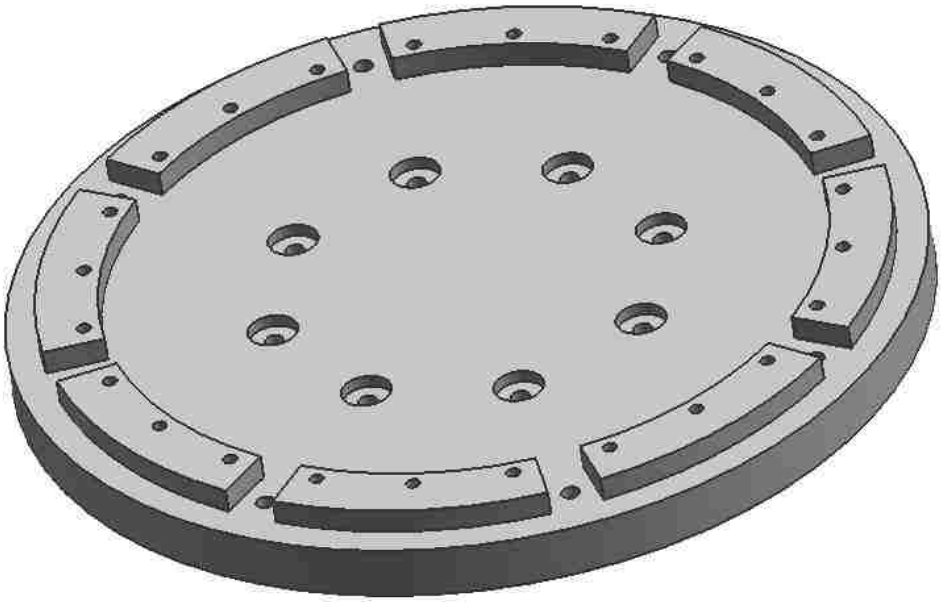

Figure 4.6. Isometric View of MR SAT Shaker Mounting Fixture

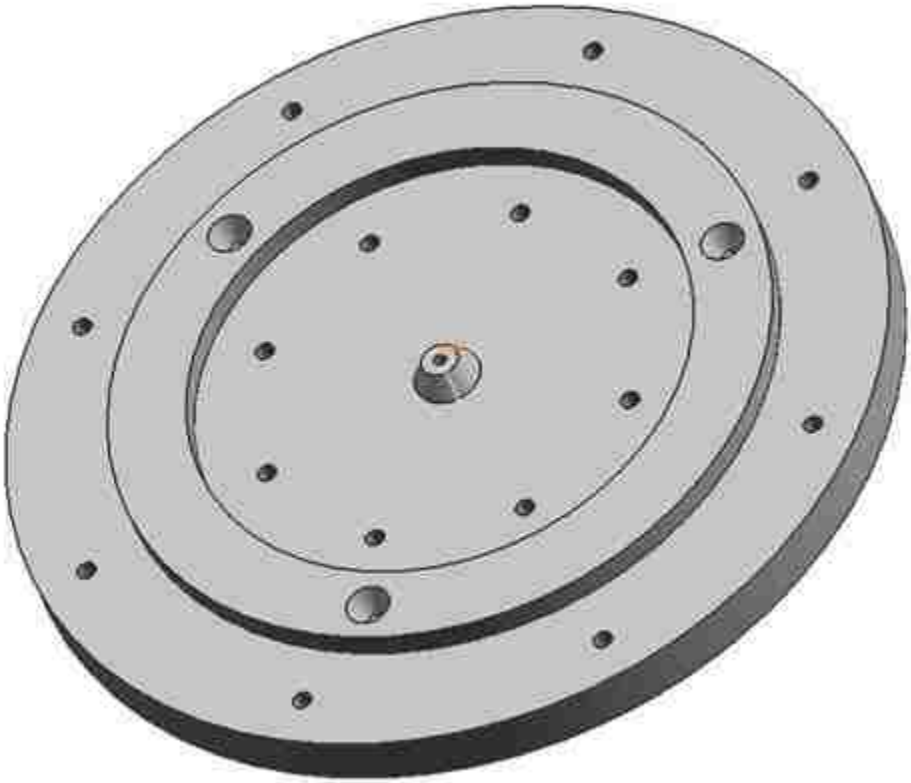

Figure 4.7. Isometric View of MRS SAT Shaker Mounting Fixture

Computer Aided Design (CAD) diagrams of the bottom plates of MR SAT and MRS SAT are shown in Figures 4.8 and 4.9, respectively. MR SAT was attached to the mounting fixture using the 24 bolt locations along the circumference of the plate, which measure 7.137 mm in diameter. Figure 4.9 indicates the locations where MRS SAT was mounted using #10 stainless steel bolts. The dimensions are given in millimeters and [inches].

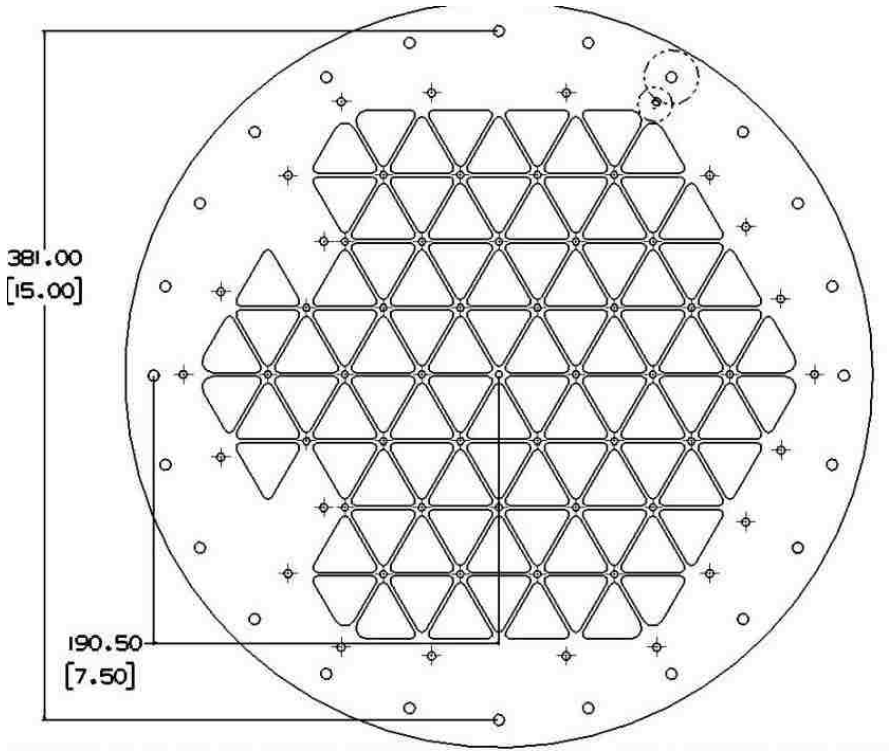

Figure 4.8. MR SAT Mounting Locations

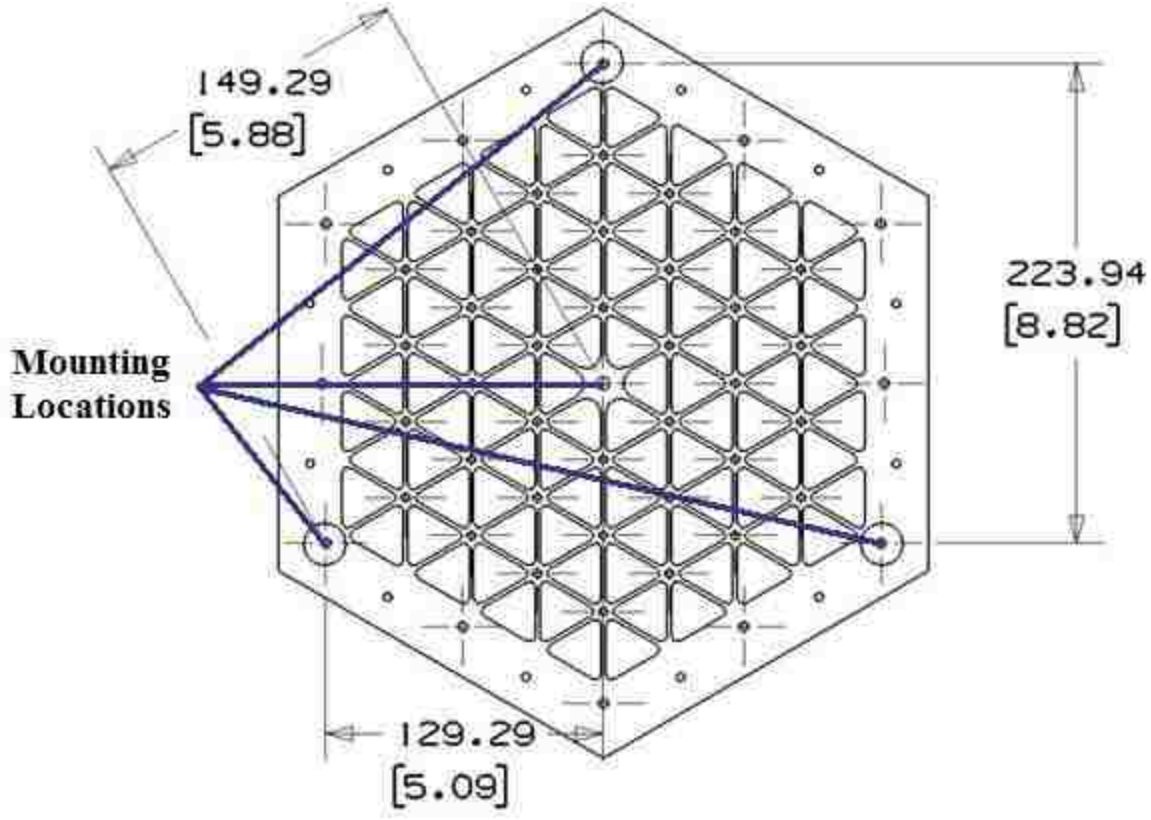

Figure 4.9. MRS SAT Mounting Locations

4.4. DATA ACQUISITION

The data acquisition system consisted of response sensors (accelerometers), signal conditioners, an input-output (I/O) board, and a computer. The functions of the digital acquisition system included:

- Measuring, conditioning, sampling, and storing the response signals and operational data of the satellites
- Processing of the measured data
- Generating drive signals for the control system
- Generating and recording the vibration responses of the satellites in an easily accessible format

Data processing was done in real time, meaning that the signals were analyzed as

they were being recorded. This allowed the spacecraft output and command signals to be accessible simultaneously as the monitoring was done. Any deviations in the excitation signal or degradation in the structure could be detected, and the automatic feedback control could be affected.

Vibration responses of the spacecraft were recorded using mono-axial piezoelectric accelerometers that were powered and signal processed by the shaker controller. The accelerometer models in this research possess an integrated circuit for signal conditioning. Thus, they require a supply power (18-30 VDC and 2-20 mA of constant current), which is a built-in feature of most modern shakers. The sensing element in the accelerometers is a crystal, which has the property of emitting a charge when subjected to a compressive force. The crystal in the accelerometer is bonded to a mass, such that when the accelerometer encounters a g-force, the mass compresses the crystal and causes it to emit a signal. The built-in circuitry then converts this charge to a voltage that is linearly proportional to acceleration. For the accelerometer models used, the sensitivity was near 10 mV/g (roughly 100 g/Volt).

The placement of the accelerometers was based on the results of the finite element analysis and the areas of interest on the spacecraft. For instance, an accelerometer was positioned on the top plate of MR SAT, as the vibrations at that location would become inputs to MRS SAT. On MR SAT, accelerometers were placed on the propulsion tank mass simulator near Panel 3 (refer to Figure 3.12), at the corner of the battery box, near the top plate on the QwkNut 3K mass simulator, and on the computer box (for the X-axis only). On MRS SAT, accelerometers were positioned on the top panel, the battery box, and the small computer box. Two control accelerometers were placed on opposite sides of the fixture, so that the average input at the center of the test article would be closest to the desired stimulus. The accelerometers were mechanically fixed to the satellites and fixture using Loctite® Threadlocker Blue 242® adhesive, which is designed for use with fasteners that require normal disassembly with standard hand tools. Several of the accelerometer locations are shown in Figures 4.10 through 4.13.

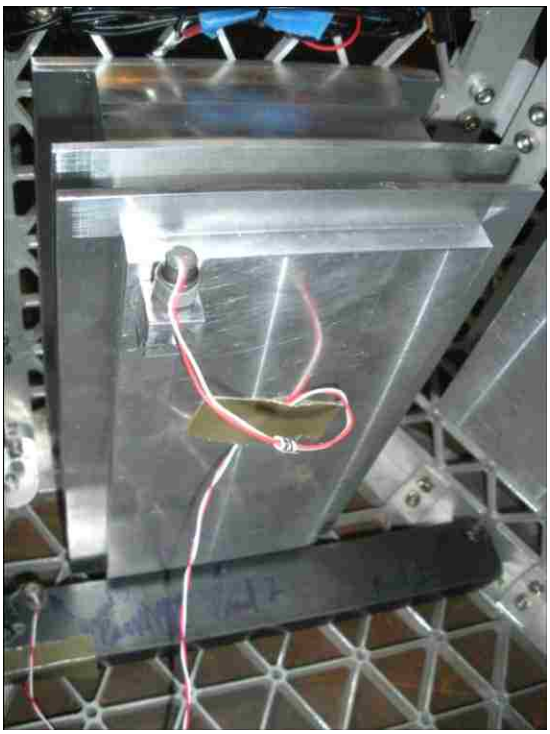

Figure 4.10. Accelerometer Mounted to the Battery Box on MR SAT Panel 2

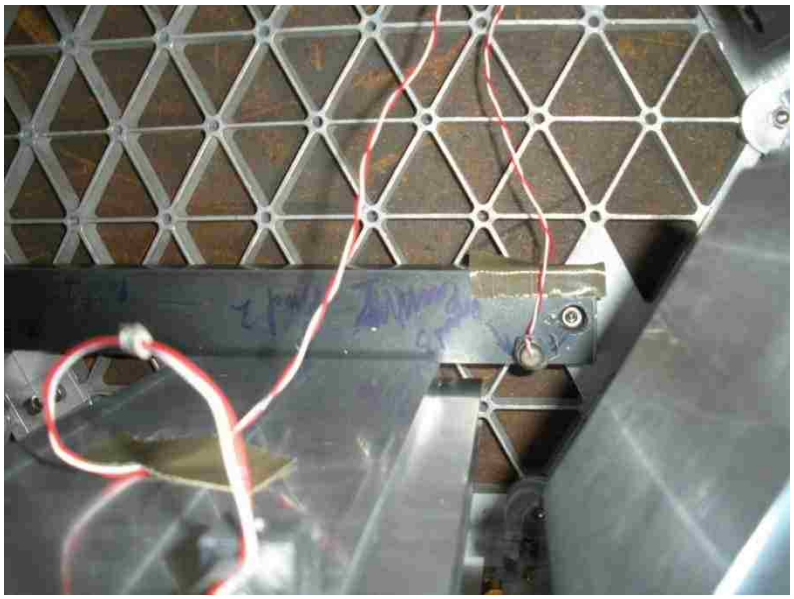

Figure 4.11. Accelerometer Mounted to the Propulsion Tank Mass Simulator on MR SAT

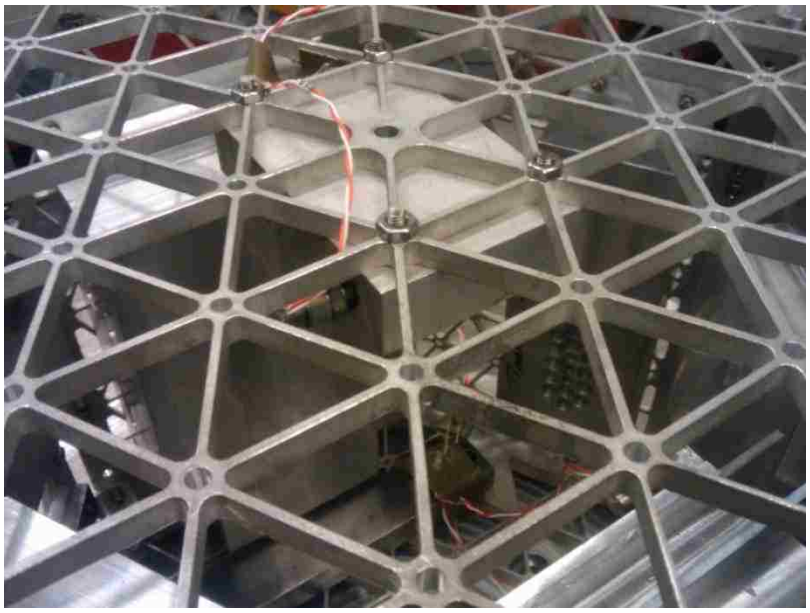

Figure 4.12. Accelerometer Mounted to the QwkNut 3K Mass Simulator on MR SAT

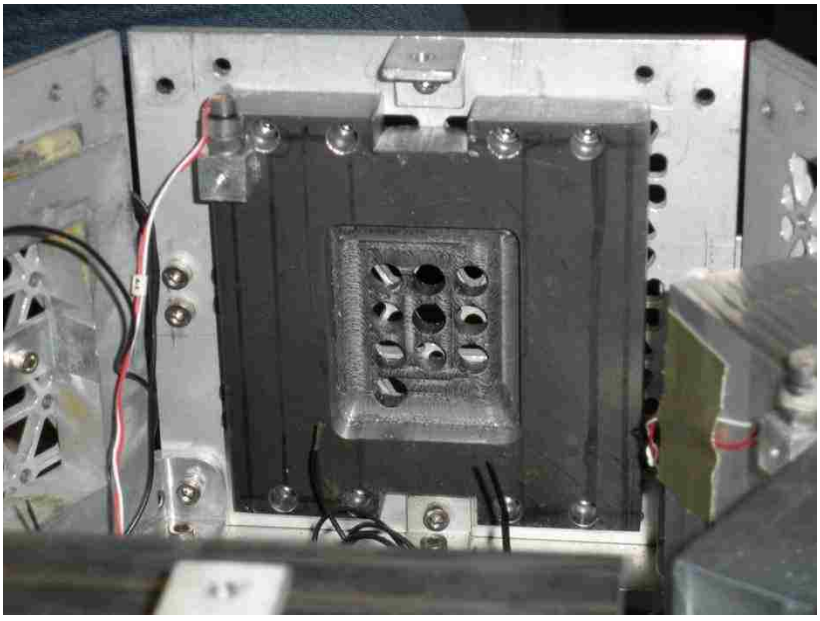

Figure 4.13. Accelerometer Mounted to the Battery Box Mass Simulator on MRS SAT

A noise reduction filter was not necessary for the random vibration tests. The shaker controller possessed a setting for automatic sample rates, which was dictated by the desired maximum test frequency (2000 Hz), and was multiplied by a factor of 2.6, which was based on digital sampling theory. However, a filter was used in the swept sine and sine burst portions of the testing. When performing both, a tracking filter was placed around the desired sinusoidal frequency. There were two potential settings for the filter, and whichever setting resulted in the smaller bandwidth was used. The first was a fractional bandwidth setting, which was a percentage of the desired sinusoidal frequency. The second was a maximum bandwidth setting, defined at a maximum value (measured in Hz). For the sine burst tests, the tracking filter settings were a fractional bandwidth of 20 percent and a maximum bandwidth of 10 Hz. Thus, for desired test frequencies at or above 50 Hz, the tracking filter would be ±5 Hz around the desired test frequency. For any desired test frequency below 50 Hz, the tracking filter width would be ±10 percent of the desired test frequency. For the swept sine tests, the tracking filter settings were a fractional bandwidth of 10 percent and a maximum bandwidth of 5 Hz. Thus, for desired test frequencies at or above 25 Hz, the tracking filter would be ±2.5 Hz around the desired test frequency. For any desired test frequency below 25 Hz, the tracking filter width would be ±5 percent of the desired test frequency.

4.5. TEST PROCEDURES

Below is a list of the procedures used for every test configuration:

1. Bolt the respective satellite mounting fixture to the shaker table head.
2. Attach the accelerometers at the predetermined locations on the satellite using Loctite® adhesive.
3. Record the accelerometer sensitivities and calibration dates.
4. Bolt the satellite to the mounting fixture.
5. Plug accelerometers into the data acquisition system.
6. Input accelerometer sensitivities and calibration dates into the Caterpillar in-house graphical programming environment for reference.
7. Input the desired test specifications for the signal generator.

8. Input the test abort limits.
9. "Run" the test using the Caterpillar in-house graphical programming environment.
10. Monitor the test activity in real-time to ensure nominal performance.
11. Perform a post-test analysis to determine if the test objectives were accomplished. If not, the probable cause of failure should be determined, and a decision should be made with regards to retesting.
12. Export the test results and graphs to a word processing and spreadsheet format for future results analysis.

For the safety of all test personnel, the following precautions were taken:

1. Ear plugs were worn when the shaker table was in operation.
2. Hard hats and protective eyewear were used in the test facility.
3. Trained Caterpillar personnel were present during a test to ensure the safe operation of the shaker table.

5. RESULTS

The experimental vibration tests discussed in this thesis were conducted in February 2010. Due to time limitations at the Caterpillar facility, only vibration tests along the X- and Z-axes were performed. The test reference frame was identical to the spacecraft reference frame shown in Figure 3.10. The plotted results can be found in the Appendix.

5.1. MR SAT

5.1.1. Z-Axis Swept Sine. Figure 1 (see Appendix) represents the acceleration profile for the initial swept sine test of the MR SAT structure from 20 Hz to 2,000 Hz. As shown in the control acceleration plot, the average of the control channels adequately tracked the demanded 0.25 g acceleration. Originally, the test limits were set to the typical default values of ±3 decibels (dB) for the alarm and ±6 dB for the abort. However, to compensate for control issues at higher frequencies due to fixture/armature resonance, these limits were widened to ±6 dB for the alarm and ±12 dB for the abort. The limits were instated to protect the test article in the event of a major deviation from the desired test level.

The swept sine test was nominal, and the plot of the response accelerometers in Figure 1 indicated that the MR SAT design exceeded the 100 Hz fundamental frequency requirement imposed by AFRL. Specifically, the fundamental natural frequency was 163.5 Hz, at which the battery box displayed the highest response with an acceleration of 3.573 g. At 572.5 Hz, the response acceleration of the propulsion tank peaked at 15.78 g; and the largest measured response overall in the system occurred in the top panel at 200.7 Hz, where the acceleration reached 48.64 g.

Apart from determining the natural frequencies of a system, another common goal of swept sine vibration tests is to determine the amplification of the excitation input from the launch vehicle interface to various components of the spacecraft -- a quantity often referred to as *transmissibility*. Assuming a single-degree-of-freedom (SDOF) configuration, which is representative of the MR SAT configuration with the shaker table, the transmissibility magnitude, T, can be expressed as

$$T = \left|\frac{Y}{X}\right| = \sqrt{\frac{k^2 + (c\omega_0)^2}{(k - m\omega_0{}^2)^2 + (c\omega_0)^2}} \qquad (5.1)$$

where ω_0 represents the forcing frequency of the system in radians per second. The parameters *k* and *c* represent the linear stiffness and linear viscous damping, respectively, while the mass of the satellite is represented by *m*. Finally, *X* and *Y* represent the input and output from the system, respectively. (The input excitation in a swept sine vibration test is a known quantity; in the present study, $X = 0.25$ g.) *Resonance* occurs when the forcing frequency is equal to the natural frequency of the system. Therefore, once the fundamental natural frequency of the satellite has been determined analytically (such as by finite element analysis), using quantities *c* and *m* of the system, the transmissibility of the response locations at resonance can be predicted.

At the fundamental natural frequency of 163.5 Hz, the transmissibility of the propulsion tank is 0.9632; the transmissibility of the battery box is 13.47; and the transmissibility of the top panel is 5.133.

5.1.2. Z-Axis Sine Burst. As described in Section 2.2, a sine burst test may be conducted to induce quasi-static qualification loads, and in doing so, verify the strength adequacy of the structure. The sine burst test was performed at a level 1.2 times limit loads at a frequency that was one-third the lowest natural frequency of the test article. The limit load requirement imposed by AFRL is 20 g's along the X-,Y-, and Z-directions, so the test was performed at a level of 24 g's. The initial swept sine test indicated that the lowest natural frequency of the MR SAT structure was 163.5 Hz, so it follows from Equation 2.3 that the test frequency should be

$$f_{sb} = \frac{f_n}{3} = 54.5\ Hz \qquad (5.2)$$

The test limits were set to ±3 dB for the alarm and ±6 dB for the abort, which are the typical default values for sine burst tests. Figure 2 in the Appendix shows the acceleration spectral density plots for the test. Recall that the ASD is useful because it

defines the distribution of average vibration energy with frequency. The square root of the integral of the ASD divided by frequency is defined as the root-mean-square (RMS) acceleration, g_{rms}, which is used to compute stress in the structure. Therefore, a large area under the ASD curve due to high peaks may be an indication that the structure will experience problems. Figure 3 represents the g_{rms} values with time for the control and response locations of the satellite.

The Z-axis sine burst test was nominal. There was no evidence of permanent deformation or damage to the test article, indicating that the MR SAT structure can withstand the anticipated static loads during flight.

5.1.3. Z-Axis Random Vibration. Random vibration consists of many frequencies occurring simultaneously, i.e. noise. These tests are conducted primarily to test and qualify spacecraft parts, such as electronic boxes or the propulsion tank, by simulating the fairing acoustic environment and rocket engine noise.

The random vibration test levels from AFRL are provided in Section 4.1. The abort limits were set to ±4 dB, and the alarm limits were set to ±2 dB. In addition, with random vibration testing, one can decide how many lines (different frequency bands) can exceed an alarm or abort limit before the test controller will sound an alarm or terminate the test. This value was set to 80 lines for both the alarm and abort levels; however, all of the random vibration tests in this research were controlled satisfactorily over their entire frequency bandwidths, so this limit was never a factor. Figures 4 and 5 in the Appendix show the acceleration spectral density and g_{rms} plots, respectively. The control plots show that the desired test levels were achieved. No permanent deformation or structural damage occurred, indicating that the MR SAT structure can withstand the anticipated random vibration loads at launch.

5.1.4. X-Axis Swept Sine. According to AFRL requirements, a swept sine test should be performed along three mutually perpendicular axes. Figure 6 in the Appendix shows the control and response acceleration during a sweep from 20 Hz to 2,000 Hz. Again, the limits were set to ±6 dB for the alarm and ±12 dB for abort. The fundamental natural frequency in the X-axis was 154.8 Hz, which exceeds the AFRL minimum stiffness requirement. At this frequency, the transmissibilities for the propulsion tank, battery box, and top panel of the test structure were 1, 5.147, and 2.591, respectively. Again, these quantities can be determined analytically using Equation (5.1).

5.1.5. X-Axis Sine Burst. The initial sine sweep indicated that the lowest natural frequency of the MR SAT structure in the X-direction was 154.8 Hz, so it follows from Equation 2.3 that the test frequency should be

$$f_{sb} = \frac{f_n}{3} = 51.6\ Hz \tag{5.3}$$

The test abort limits were set to the typical default value of ±3 dB for the alarm and ±6 dB for the abort. Figure 7 in the Appendix shows the acceleration spectral density plots for the control and response locations. The input acceleration is, once again, the average of the control accelerometers. Figure 8 represents the g_{rms} values with time for the control and response locations of the satellite.

The X-axis sine burst test was nominal. There was no evidence of permanent deformation or damage to the test article, indicating that the MR SAT structure can withstand the anticipated static loads during flight.

5.1.6. X-Axis Random Vibration. The random vibration test levels are provided in Section 4.1. The abort limits were set to ±4 decibels, while the alarm limits were set to ±2 decibels. Figure 9 in the Appendix shows the acceleration spectral density plots at the response and average control locations on the satellite; the latter shows that the desired test levels were achieved. The root-mean-square acceleration plots are provided in Figure 10. The control g_{rms} plot indicates that the overall g_{rms} is approximately 9.24, as desired. Since no permanent deformation or structural damage occurred, the test indicates that MR SAT can withstand the anticipated random vibration loads in the X-axis during launch.

5.2. MRS SAT

Due to time constraints on the test day, the team had to forgo the random vibration and X-axis vibration tests for MRS SAT.

5.2.1. Z-Axis Swept Sine. The acceleration plots at the response and average control locations of the MRS SAT test structure for the Z-axis swept sine test are plotted in Figure 11 in the Appendix. The test limits were set to ±6 dB for the alarm and ±12 dB for the abort. The fundamental natural frequency was 236.4 Hz, which exceeds AFRL stiffness requirements. At this frequency, the transmissibilities for the top panel, battery box, and small computer box of the test structure were 7.918, 5.481, and 1.701, respectively.

5.2.2. Z-Axis Sine Burst. The initial sine sweep indicated that the lowest natural frequency of the MRS SAT structure was 236.4 Hz, so it follows from Equation 2.3 that the test frequency should be

$$f_{sb} = \frac{f_n}{3} = 78.8\ Hz \tag{5.4}$$

The test limits were set to the typical default values of ±3 dB for the alarm and ±6 dB for the abort. Figure 12 in the Appendix shows the acceleration spectral density plots for the response and average control accelerometers on the satellite, and Figure 13 shows the root-mean-square acceleration plots. There was no evidence of permanent

deformation or damage to the test article, which indicates that the MRS SAT structure can withstand the anticipated static loads during flight

5.3. MR AND MRS SAT DOCKED

As mentioned in Section 3.4.3, it is a system-level requirement that MR and MRS SAT remain docked until separation on orbit. At the time of this research, the spacecraft design called for one non-explosive actuator (NEA) device attached to the top panel of MR SAT and a Bolt Retractor mechanism attached to the bottom panel of MRS SAT to prevent the connection bolt from being discharged into MRS SAT following release of the NEA device. Also, to circumvent the need for a flatness requirement on the bottom panel of MRS SAT and the top panel of MR SAT, the satellites only made contact at three points that were separated by 120 degrees.

During the vibration testing of the MR and MRS SAT docked configuration, it was discovered that the interface shown in Figure 3.11 resulted in severe rattling in the cup/cone arrangement because the satellites were not rigidly joined by the NEA device. To avoid damage to the spacecraft, the test was aborted. A decision was made to forgo retesting of the MR and MRS SAT docked configuration, so no results were obtained. The potential solutions to this design problem are discussed in Section 6 under Lessons Learned.

5.4. FINITE ELEMENT ANALYSIS COMPARISON

A finite element model was created by the M-SAT team for MR SAT prior to the shaker table tests, which predicted a fundamental natural frequency of 234 Hz. When compared to the experimentally determined result of 163.5 Hz for the Z-direction swept sine test, the error in the model is 43.12 percent. One explanation for the discrepancy is that the model does not consider losses and damping. The damped natural frequency is related to the undamped natural frequency by

$$f_{damping} = f_n \sqrt{1-\zeta^2} \qquad (5.5)$$

where ζ represents the damping ratio and f_n is the undamped natural frequency. Using

equation (5.7), the damping ratio works out to be 0.72 for MR SAT, while typical industry values range from 0.5 to 0.7. The calculated ratio may be slightly high, in part, because the finite element model does not consider joints, but treats the satellite as if all connections are uniform. Also, the model uses two-dimensional, rather than three-dimensional, elements, such that the thickness is neglected. An enhanced finite element model, which will consider loss and damping factors, is currently under development by a student at Missouri S&T.

6. CONCLUSION

Despite advanced and thorough preparation, the vibration testing of the M-SAT spacecraft was not without challenges. The issues that arose were difficult to anticipate and led to delays in the test schedule. A few of these challenges and the lessons learned are discussed below.

6.1. LESSONS LEARNED

6.1.1. Fixture Design. As mentioned in Section 2.4, the configuration between the shaker table and the satellites required the use of an adaptor plate, and it was important that the team communicated with the Caterpillar facility personnel during this design process. Open communication was necessary, not only to ensure compatibility between the fixture and the shaker table mounting locations, but also because the fixture design can affect the test item vibration results. Just as the launch vehicle and spacecraft must be treated as a system when analyzing the load environments during flight, the characteristics of the mounting fixture, shaker table armature, and test item must be considered jointly.

The goal in designing the mounting fixtures for MR and MRS SAT was to simulate, as closely as possible, the mechanical interfaces for the flight configuration. Although the adaptor plate designs were approved by Caterpillar personnel prior to their manufacture, the team still encountered issues with armature/fixture resonance that caused control issues at higher frequencies during the initial MR SAT swept sine test. This problem led to significant delays in the test schedule. The remoteness of the test site from the Missouri S&T campus prevented the M-SAT team from performing a pre-test, but this experience reinforced the significance of checking the test item and adaptor plate with the shaker table in advance of the tests.

6.1.2. Equipment Operation. A good practice is to limit the working hours to a standard day when possible, and to avoid the most dangerous, high-level tests late at night or first thing in the morning. The M-SAT test schedule originally allotted one day for the shaker table tests. However, delays resulting from the armature/fixture resonance discussed above prevented the team from maintaining this schedule, and also led to performing several of the most severe tests late in the day. In this case, it would have been beneficial to perform a pre-test as a "dry run" for working out any unforeseen problems with the equipment. Furthermore, this would have provided an idea of the necessary time frame for completing the tests.

6.1.3. Design Iterations. One of the most important aspects of test planning is the pre-test analysis, because it offers insight into the expected response of the spacecraft to a particular input, as well as the knowledge to deal with it in advance of the test. This allows the actual test process to go much faster and permits the attention during the test to focus on new problems that could not be anticipated. The structures of both MR and MRS SAT survived the shaker table tests and met the design requirements set forth by AFRL. The stiffness requirements were achieved, and there was no damage to the spacecraft. However, the testing of the docked configuration pointed out an inherent flaw in the design of the mechanical interface between the satellites, as discussed in Section 5.3. This is an excellent example of the mutual relationship between analytical and experimental methods in structural dynamics. Environmental tests can reveal problems in the design that are not readily determined by analysis.

Specifically, during the vibration testing of the MR and MRS SAT docked configuration, it was discovered that the interface shown in Figure 3.11 resulted in severe rattling in the cup / cone arrangement because the satellites were not rigidly joined by the NEA device. One possible solution to this problem is to use three NEA devices separated by 120 degrees to connect the top plate of MR SAT to the bottom plate of MRS SAT. This would increase the stiffness between the satellites; however, the cost of adding two QwkNut 3K and Bolt Retractor mechanisms would be significant for a university project.

Another solution is to redesign the MRS SAT structure. Following the vibration tests in February 2010, the M-SAT team determined it was unnecessary to include torque coils for attitude control in the MRS SAT structure because the satellite was already

equipped with a Bluetooth antenna that would serve in this function. Therefore, the MRS SAT structure was altered to resemble two smaller cube satellites.

Cubesats are designed to be small and uniform spacecraft that can perform a variety of mission operations. While their standard size measures 10x10x10 cm (1U), there are variations to include a 10x10x20 cm (2U) version and a 10x10x30 cm (3U) version. The reason for the prescribed structure is due to its deployment method -- typically a P-POD (Poly Picosatellite Orbital Deployer) -- which is generally a rectangular metal box, lined with guide rails along the inside. The cube satellites are housed in the P-POD during launch, and when the desired orbit is reached, a signal is given to the P-POD to simultaneously open the door at the front and release a spring at the back. This in turn pushes the satellites along the guide tracks and out of the launcher. Unlike the NEA device, they do not impart any rotational inertia to the cube satellite during deployment. Since the P-POD is extremely precise and well-proven in low-Earth orbit, it is widely used both by commercial and government organizations in the industry [21].

6.2. CONTINUING WORK

The M-SAT team recently submitted a proposal for the 2011-2013 Nanosat-7 competition, and was invited to compete again by University Nanosat Program officials. The team proposed a modified mission that will conduct spacecraft proximity operations, while continuing the technology demonstration objectives of previous campaigns.

Both the DoD and NASA have expressed interest in using spacecraft for the surveillance of resident space objects (RSOs), which may include "friendly" or "adversarial" spacecraft or naturally-occurring/human space debris. The proposed research would include a primary inspector spacecraft similar to the Nanosat-6 MR SAT. However, the new structure will be configured as a hexagonal prism with triangular isogrid panels to reduce mass. The inspector spacecraft will be used to deploy two cubesats, and then conduct autonomous proximity operations about the cubesats that align with AFRL's key research interests [21].

A finite element model of the Nanosat-6 structure was being developed by Missouri S&T students during the Fall 2010 semester, and additional vibration tests were

conducted at the Caterpillar facility in Peoria, Illinois, to verify the analysis. The new structural design will draw heavily from lessons learned during the Nanosat-6 competition. Missouri S&T is currently installing its own shaker, and the assistance the team continues to receive from Caterpillar will be of great advantage in establishing the capabilities to perform these tests on campus in the near future.

6.3. CLOSING REMARKS

This thesis documents the shaker table testing of a microsatellite system, including the purpose and philosophy of experimental methods in structural dynamics, the design of the test structure, and integration with the shaker table. The results show that the MR and MRS SAT structures meet the stiffness requirements set forth by AFRL, while keeping within mass and volume restrictions. The lessons learned were presented to offer insight for future shaker table tests. Some of the challenges met by the M-SAT team are likely typical to those of any small satellite program. In the present culture of "faster, better, cheaper," the trend in the aerospace industry is to rely more on analysis and less on structural tests. The findings of this research confirm that only a well-balanced test program can instill confidence in delivered hardware.

APPENDIX

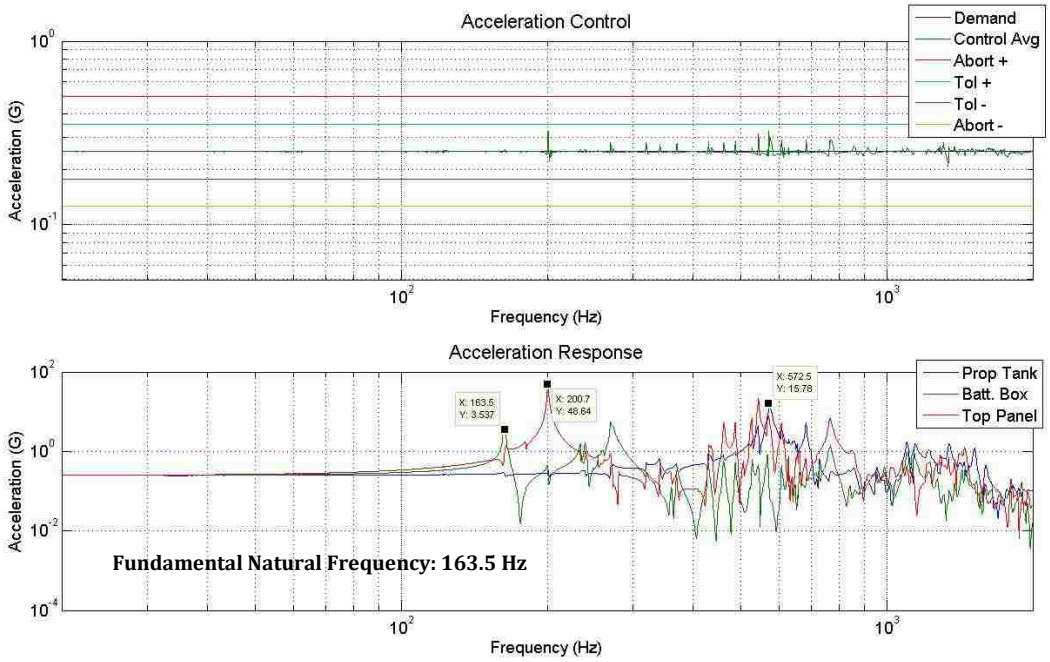

Figure 1. MR SAT Z-Axis Swept Sine Acceleration Plots

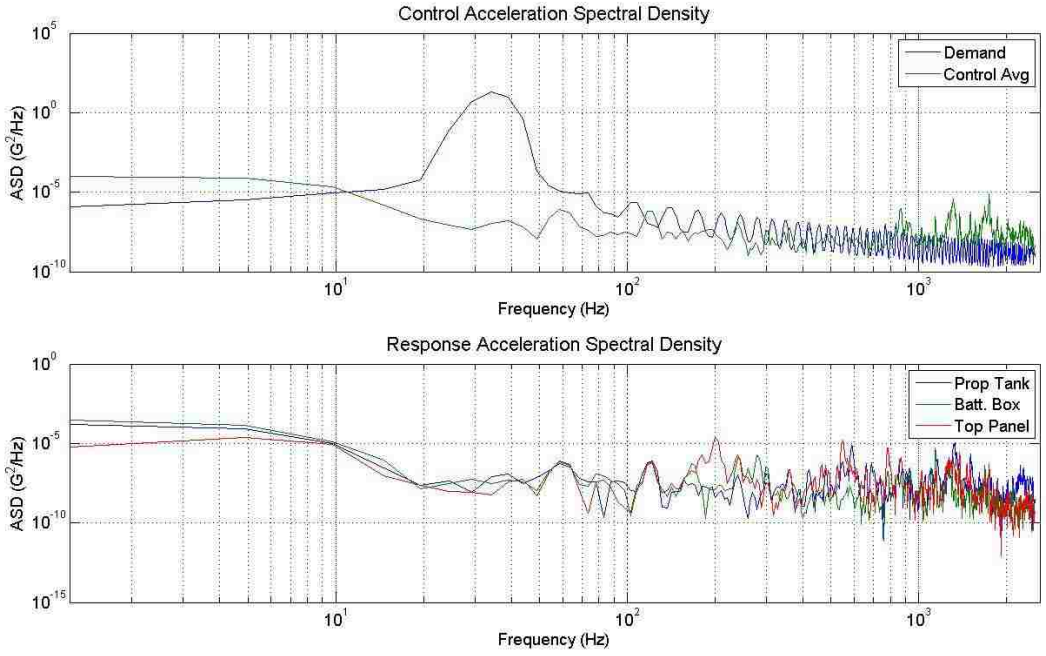

Figure 2. MR SAT Z-Axis Sine Burst Acceleration Spectral Density Plots

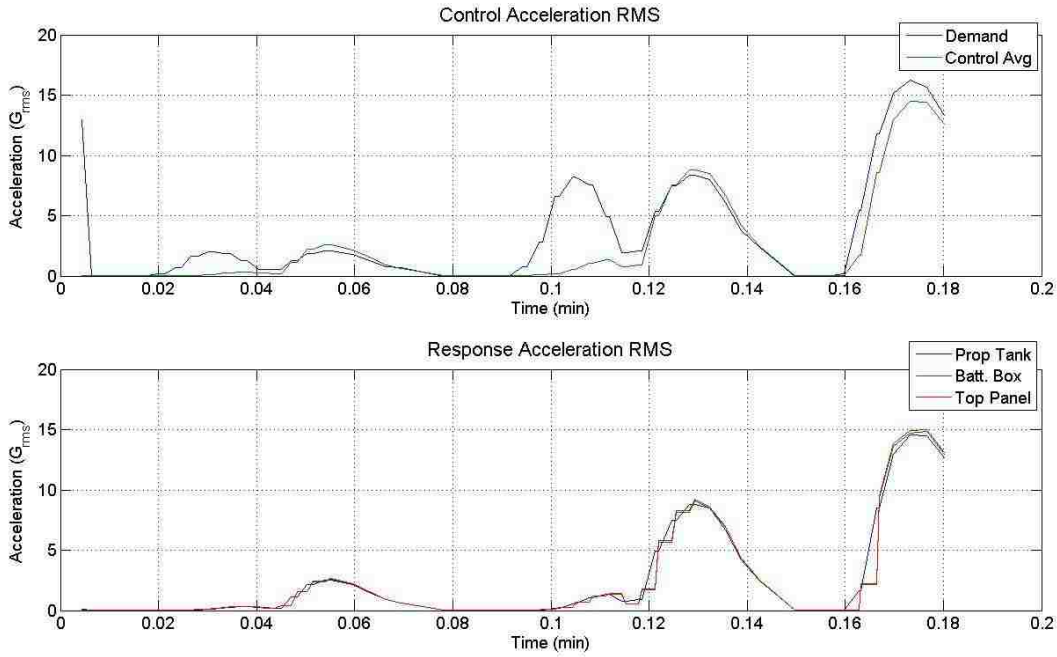

Figure 3. MR SAT Z-Axis Sine Burst Acceleration RMS Plots

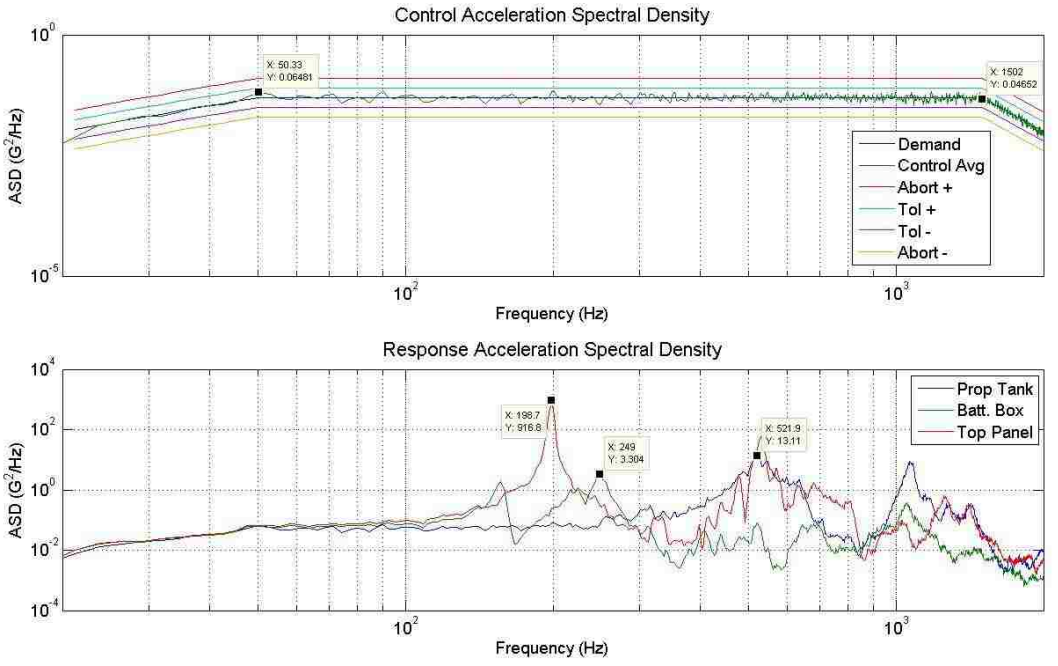

Figure 4. MR SAT Z-Axis Random Vibration Acceleration Spectral Density Plots

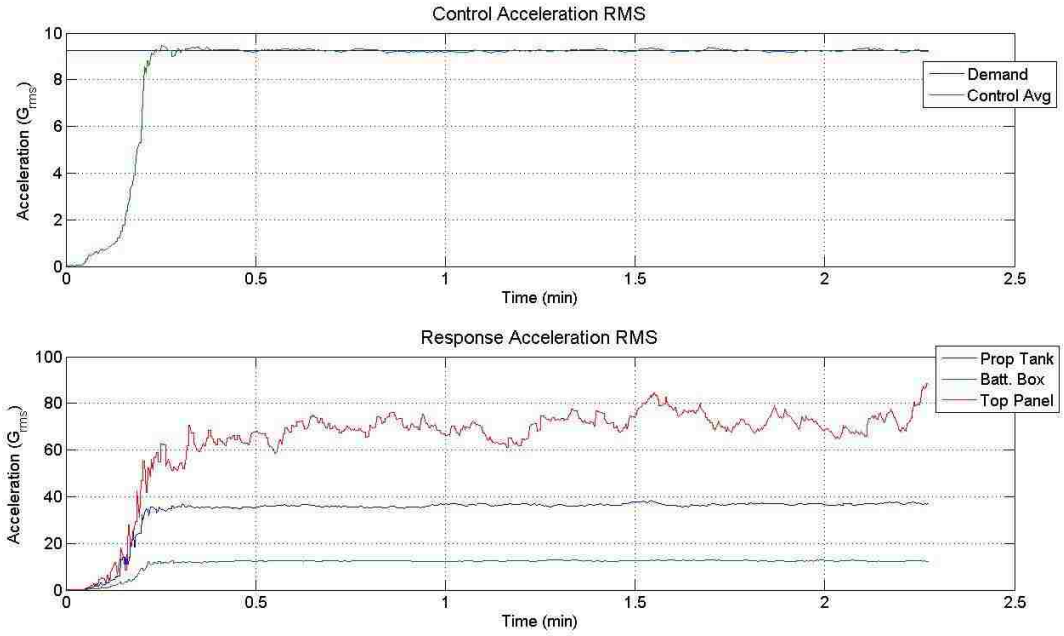

Figure 5. MR SAT Z-Axis Random Vibration Acceleration RMS Plots

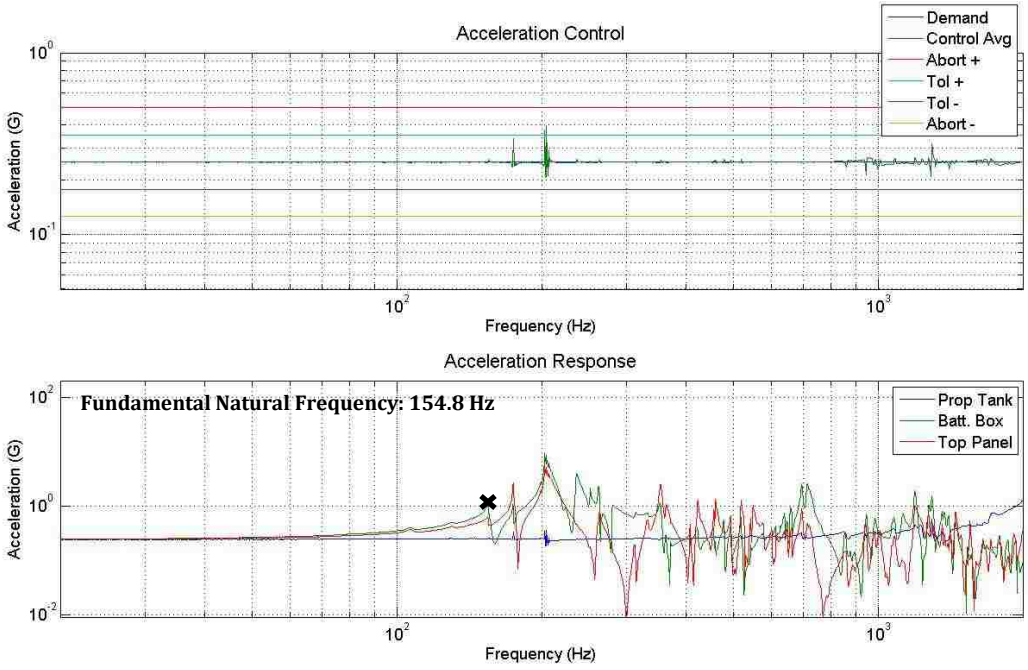

Figure 6. MR SAT X-Axis Swept Sine Acceleration Plots

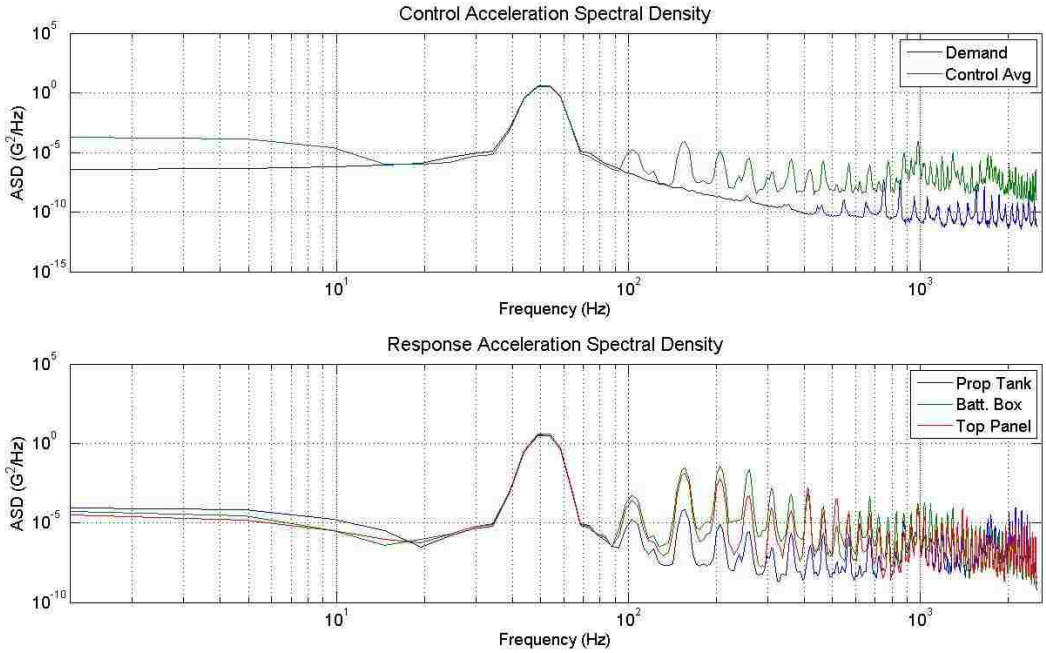

Figure 7. MR SAT X-Axis Sine Burst Acceleration Spectral Density Plots

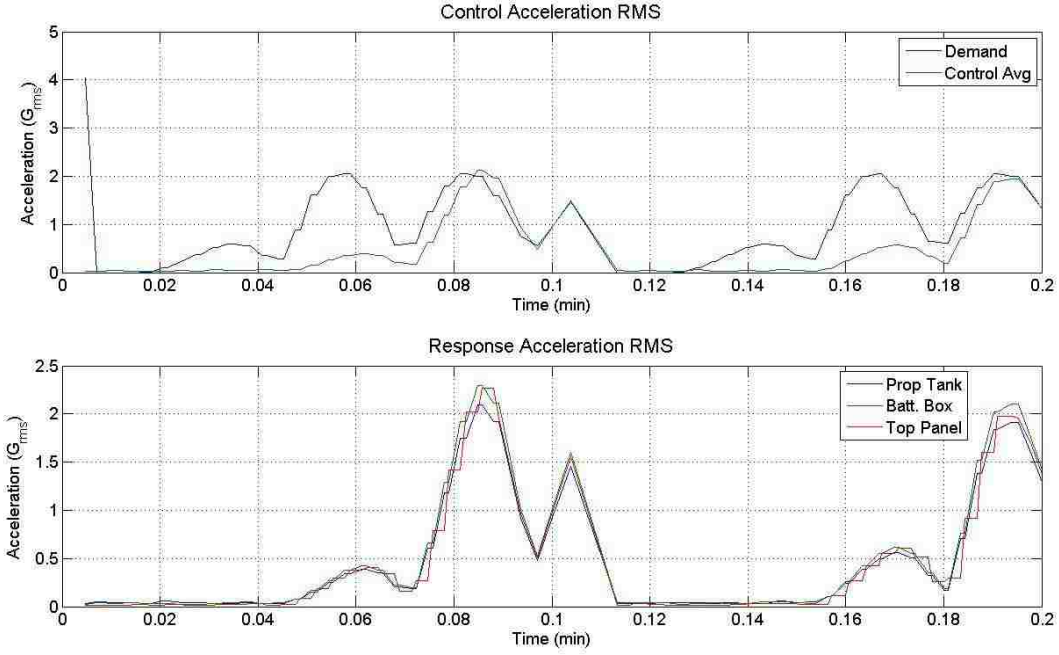

Figure 8. MR SAT X-Axis Sine Burst Acceleration RMS Plots

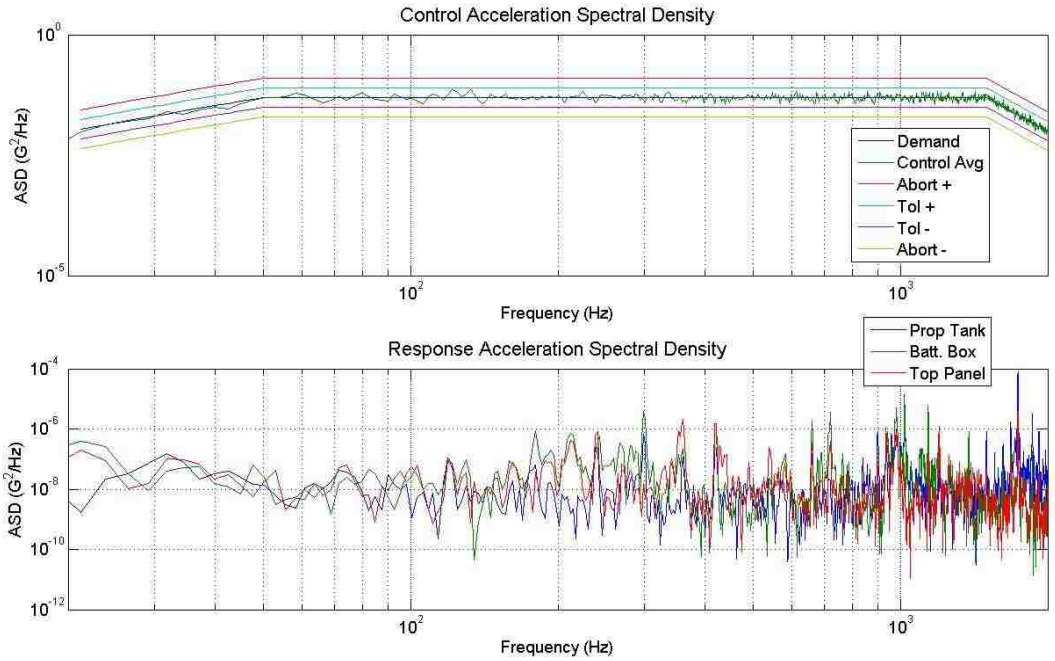

Figure 9. MR SAT X-Axis Random Vibration Acceleration Spectral Density Plots

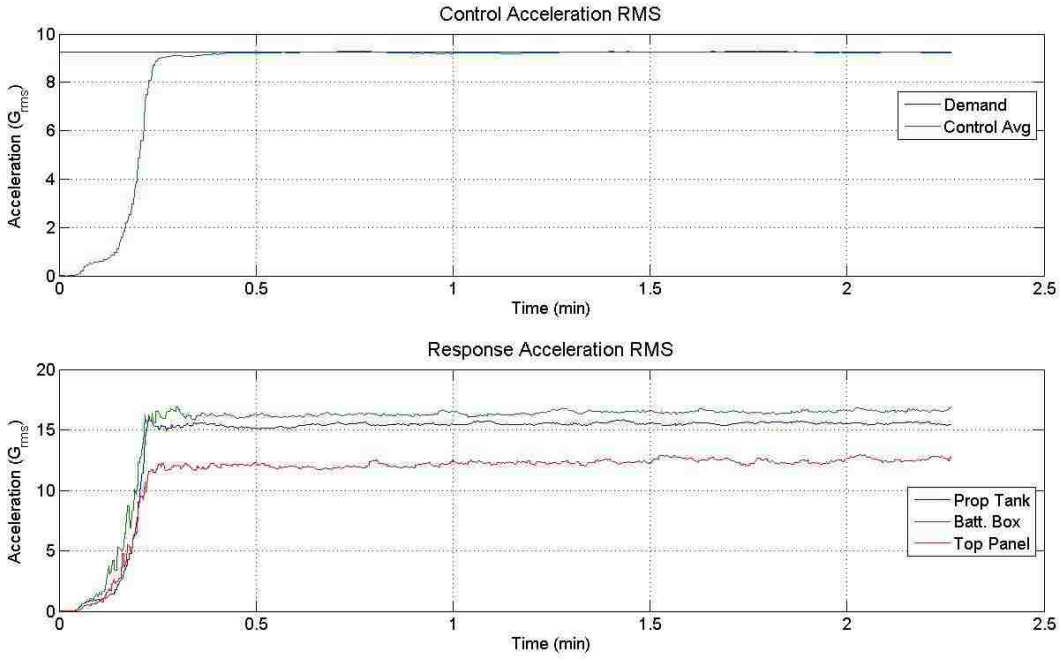

Figure 10. MR SAT X-Axis Random Vibration Acceleration RMS Plots

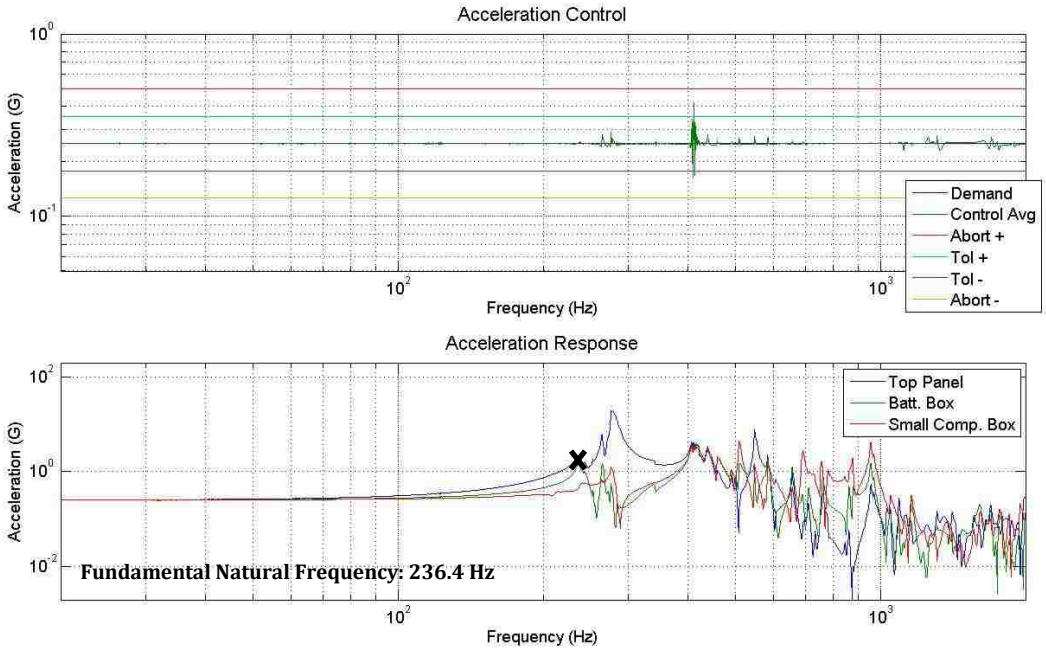

Figure 11. MRS SAT Z-Axis Swept Sine Acceleration Plots

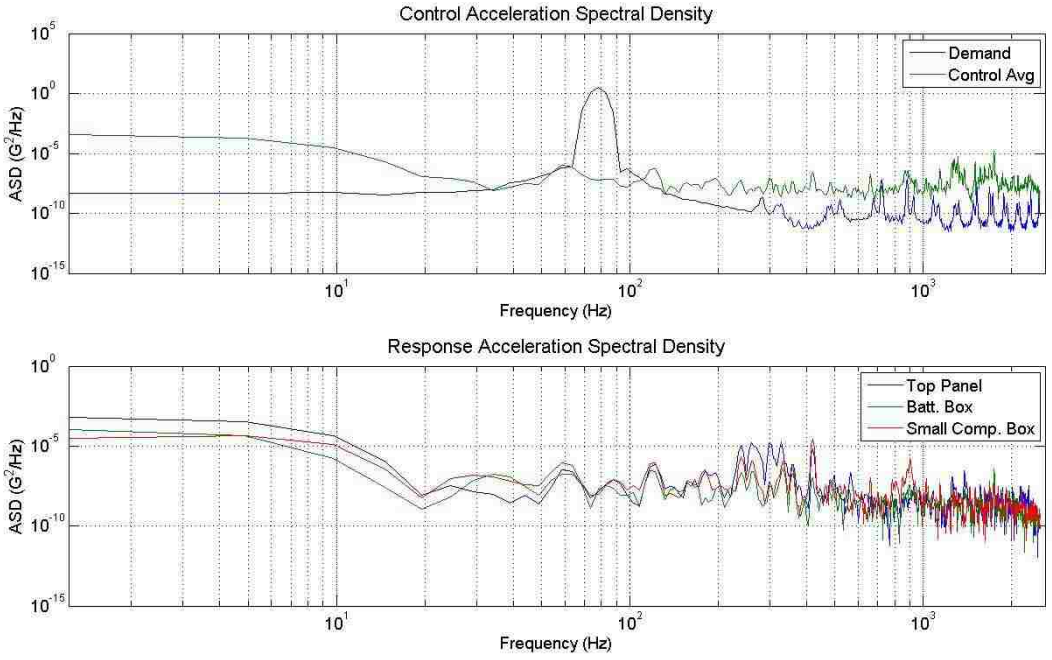

Figure 12. MRS SAT Z-Axis Sine Burst Acceleration Spectral Density Plots

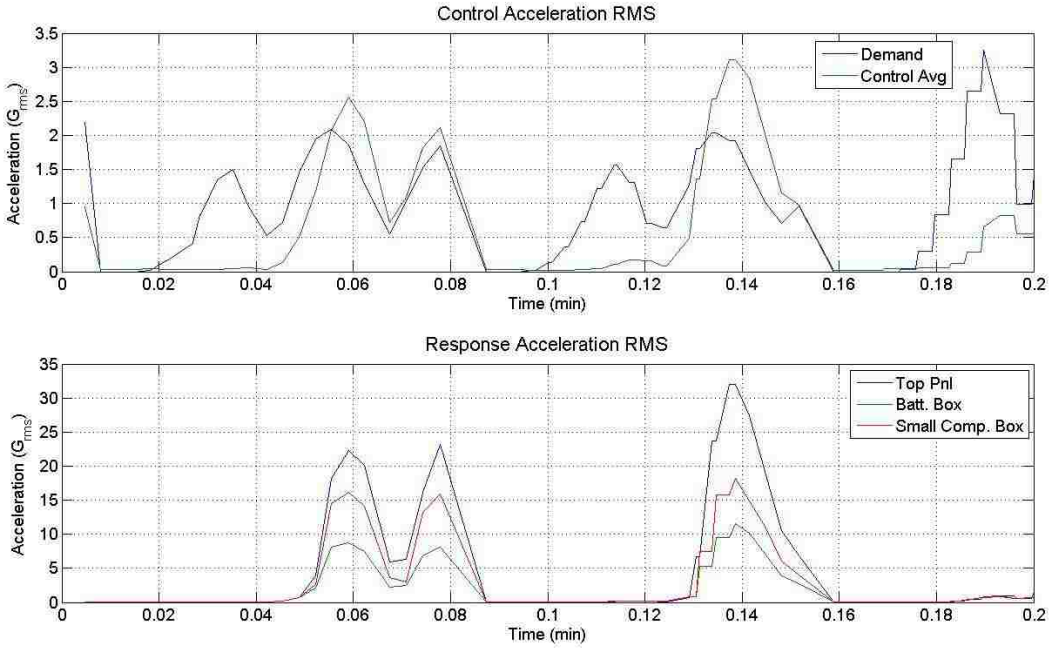

Figure 13. MRS SAT Z-Axis Sine Burst Acceleration RMS Plots

BIBLIOGRAPHY

[1] Jacob Job Wijker, *Spacecraft Structures*, 1st Ed., Springer: New York (2008).

[2] Jorge P. Arenas and Ravi N. Margasahayam, "Noise and Vibration of Spacecraft Structures," *Revista Chilena de Ingeniería*, Vol. 14, No. 3, Pp. 251-264 (2006).

[3] NASA Space Vehicle Design Criteria (Structures), *Structural Vibration Prediction*, NASA SP-8050, June 1970.

[4] Loretta Hidalgo Whitesides, Aug. 19, 2008, "NASA Releases Plan for Ares I Vibration Problem," Wired Science website, June 22, 2010. http://www.wired.com/.

[5] NASA Technical Standard, *Load Analyses of Spacecraft and Payloads*, NASA-STD-5002, June 21, 1996.

[6] Terry C. Fisher and W.J. Marner, "Forging New Partnerships through the Use of Environmental Test Facilities," ITEA Conference, Tullahoma, TN, Oct. 12-15, 1999.

[7] Anatoly Zak, Oct. 2, 2007, "Shortcut to Simplest Satellite," Russian Space Web website, Oct. 13, 2010. http://www.russianspaceweb.com/sputnik_design.html.

[8] NASA, Jan. 30, 2008, "Explorer 1 Overview," NASA website, Oct. 13, 2010. http://www.nasa.gov/mission_pages/explorer/explorer-overview.html.

[9] U.S. Army, "The Redstone Test Stand," Redstone Arsenal Historical Information website, Oct. 13, 2010. http://www.redstone.army.mil/history/teststand/welcome.html.

[10] Mark Wade, "R-7," Encyclopedia Astronautica website, June 22, 2010. http://www.astronautix.com/lvs/r7.htm.

[11] National Park Service, "Propulsion and Structural Test Facility," National Park Service website, Oct. 13, 2010. http://www.nps.gov/history/history/online_books/butowsky4/space9.htm.

[12] National Park Service, "Saturn V Dynamic Test Stand," National Park Service website, Oct. 13, 2010. http://www.nps.gov/history/history/online_books/butowsky4/space11.htm.

[13] NASA, "Space Shuttle Enterprise Lifted into Dynamic Test Stand," NASA Images website, June 22, 2010. http://www.nasaimages.org/.

[14] Scott H. Simpkinson, "Testing to Ensure Mission Success," *What Made Apollo a Success?*, NASA SP-287, 1971, NASA Office of Logic Design website, Oct. 13, 2010. http://klabs.org/history/reports/sp287/ch3.htm.

[15] NASA, "Shuttle Vibration Forces Experiment," May 5, 1999, Shuttle Press Kit website, June 22, 2010. http://www.shuttlepresskit.com/sts-96/payload25.htm.

[16] *Vibration Monitoring, Testing, and Instrumentation*, Ed. Clarence W. de Silva, CRC Press, LLC.: Boca Raton, FL, 2007.

[17] John H. Leete, "Structural Dynamics," in *Space Vehicle Mechanisms*, Ed. Peter L. Conley, John Wiley & Sons, Inc.: New York, Pp. 579-619, 1998.

[18] Dennis L. Kern and Terry D. Scharton, "NASA Handbook for Spacecraft Structural Dynamics Testing," 5th International Symposium on Environmental Testing for Space Programmes, Noordwijk, The Netherlands, June 15, 2004.

[19] Terry D. Scharton, "Vibration and Acoustic Testing of Spacecraft," *Sound and Vibration*, June 2002.

[20] AFRL/VSSV, University Nanosat-6 Program, "Nanosat-6 User's Guide," (Limited Release) UN6-0001 – Rev A, University Nanosat Program Office, Kirtland AFB, NM.

[21] Henry J. Pernicka, Missouri S&T Satellite Team, "Design, Fabrication, and Test of Spacecraft Conducting Proximity Operations," Missouri University of Science and Technology, Rolla, MO, 2010.

VITA

Tonya Michelle Sanders was born in Kansas City, Missouri, to Harold and Sandra Sanders. She has one younger sibling, Kathy. Tonya graduated in May 2003 from Blue Ridge Christian School, and enrolled in Longview Community College in the fall. She transferred to the University of Missouri - Rolla, now Missouri University of Science and Technology, in August 2005, where she earned a Bachelor of Science degree in Aerospace Engineering in May 2008. Tonya continued at Missouri S&T, graduating in May 2011 with a Master of Science degree in Aerospace Engineering.

At Missouri S&T, Tonya was a member of Tau Beta Pi (the Engineering Honor Society) and Sigma Gamma Tau (the Aerospace Engineering Honor Society). She was Vice President and Treasurer of the Miners in Space microgravity team, participating in research on NASA's reduced gravity aircraft in 2007 and 2008. Tonya has held internships at Goddard Space Flight Center and Dryden Flight Research Center. While a graduate student, she was offered the Chancellor's Fellowship and was a Graduate Teaching Assistant for the Mechanical Engineering *Introduction to Design* course.